ANL-6973

Argonne National Laboratory

ENGINEERING DEVELOPMENT OF FLUID-BED FLUORIDE VOLATILITY PROCESSES

Part 8. Pilot-plant Development of a Process for Uranium Alloy Fuels

by

John T. Holmes, Howard Stethers,
and John J. Barghusen

Printed in USA. Price $3.00. Available from the Clearinghouse for Federal Scientific and Technical Information, National Bureau of Standards, U. S. Department of Commerce, Springfield, Virginia

ANL-6973
Chemical Separations
Processes for
Plutonium and Uranium
(TID-4500, 47th Ed.)
AEC Research and
Development Report

ARGONNE NATIONAL LABORATORY
9700 South Cass Avenue
Argonne, Illinois 60440

ENGINEERING DEVELOPMENT OF FLUID-BED FLUORIDE VOLATILITY PROCESSES

Part 8. Pilot-plant Development of a Process for Uranium Alloy Fuels

by

John T. Holmes, Howard Stethers,
and John J. Barghusen

Chemical Engineering Division

August 1965

Operated by The University of Chicago
under
Contract W-31-109-eng-38
with the
U. S. Atomic Energy Commission

Other reports in this series:

Part 1: Bench-scale Investigation of a Process for Zirconium-Uranium Alloy Fuel, by D. Ramaswami, N. M. Levitz, J. T. Holmes, and A. A. Jonke (ANL-6829)

Part 2: Bench-scale Investigation of a Process for Aluminum-Uranium Alloy and Stainless Steel-Cermet Fuels, by D. Ramaswami, N. M. Levitz, and A. A. Jonke (ANL-6830)

Part 3: Fluid-bed Fluorination of Uranium Dioxide Fuel Pellets, by L. J. Anastasia, J. D. Gabor, and W. J. Mecham (ANL-6898)

Part 4: Fluidized-packed Beds: Studies of Heat Transfer, Solids-Gas Mixing, and Elutriation, by J. D. Gabor and W. J. Mecham (ANL-6859)

Part 5: Description of a Pilot-scale Facility for Uranium Dioxide-Plutonium Dioxide Fuel Processing Studies, by G. J. Vogel, E. L. Carls, and W. J. Mecham (ANL-6901)

Part 6: Preparation of Dense Uranium Dioxide Particles from Uranium Hexafluoride in a Fluidized Bed, by I. E. Knudsen, N. M. Levitz, and A. A. Jonke (ANL-6902)

Part 7: The Corrosion of Nickel in Process Environments, by A. A. Chilenskas.and G. E. Gunderson (ANL-6979)

Part 9: Computer Programs for Alloy-fuel Process Calculations, by J. T. Holmes and D. Ramaswami (ANL-6992)

Part 10: Bench-scale Studies on Irradiated Highly-enriched Uranium Alloy Fuels, by A. A. Chilenskas and K. S. Turner (ANL-6994)

TABLE OF CONTENTS

TABLE OF CONTENTS

LIST OF FIGURES

LIST OF FIGURES

LIST OF TABLES

LIST OF TABLES

ENGINEERING DEVELOPMENT OF FLUID-BED FLUORIDE VOLATILITY PROCESSES

Part 8. Pilot-plant Development of a Process for Uranium Alloy Fuels

by

John T. Holmes, Howard Stethers, and John J. Barghusen

SUMMARY

A fluid-bed fluoride volatility (FBV) process for the recovery of uranium from highly-enriched uranium-Zircaloy-2 (U-Zr) and uranium-aluminum (U-Al) alloy fuels has been developed on a pilot-plant scale. The conceptual operation of the process consists of three major steps: a hydrochlorination step, in which alloying materials are separated by virtue of the volatility of their chlorides; a fluorination step, in which the uranium is volatilized and recovered as the hexafluoride; and a final product-decontamination step. The first two reactions are conducted in a single vessel (halogenation reactor) in which a bed of inert alumina particulate material is fluidized by the reagent gases. The use of a fluid bed facilitates dissipation of the reaction heat. An important feature of this process is the use of a packed bed of alumina particulate materials as a high-temperature filter.

In the first step, the alloying elements and cladding of the fuel are separated from the uranium by converting them into chlorides by reaction with gaseous HCl. These alloy-metal chlorides are volatile at the reaction temperature; the uranium chlorides are relatively nonvolatile and remain in the reactor system. The volatile alloy-metal chlorides are reacted with steam in a second fluid-bed reactor (pyrohydrolysis reactor) to form waste solid oxides. Particulate uranium chlorides entrained from the halogenation reactor by the exit gas stream are retained by the packed-bed filter. In the recovery step, the uranium compounds in both the fluid-bed and packed-bed filter are reacted with gaseous anhydrous hydrogen fluoride and then fluorine, and the product UF_6 is recovered by sorption on beds of NaF at 100°C. Product decontamination can be achieved by distillation or sorption-desorption from NaF.

This report summarizes pilot-plant development work pertaining to the hydrochlorination and fluorination of unirradiated U-Zr and U-Al alloy. Recoveries of more than 99% of the uranium, high reaction rates, and high reagent utilization efficiencies were demonstrated in a total of 18 pilot-plant experiments involving the processing of up to 56 kg of simulated zirconium

fuel and up to 18 kg of simulated aluminum fuel in single runs. Recommended operating conditions for processing both fuel types are as follows:

1. A hydrochlorination step, with the fuel element immersed in a fluidized bed, to separate the alloying metals from the uranium.

	U-Zr	U-Al
	Temperatures (°C)	
Halogenation reactor	350-450	300-350
Packed-bed filter	350	200
Pyrohydrolysis reactor	350	350
	Concentration of HCl in N_2 (v/o)	
	80	80

2. A hydrofluorination step, to convert the uranium chlorides to fluorides by using 20-25 v/o HF in N_2 at 350°C.

3. A fluorination step, to recover the uranium as UF_6, involving a gradual increase in temperature of the halogenation reactor and packed-bed filter from 250 to 500°C, while fluidizing with 1.0 to 5 v/o fluorine in nitrogen; then gradual increase in fluorine concentration to 60-80 v/o. The alumina particulate material may be maintained static during the latter period.

Uranium losses were due to two mechanisms: (1) entrainment of particulate uranium compounds and volatilization of uranium chlorides in the gas stream during the hydrochlorination step, and (2) retention of uranium by alumina bed material at the end of the fluorination step. These uranium losses were as low as 0.2% during hydrochlorination, and that retained by alumina was as low as 0.25% of the uranium in the initial fuel charge.

Nickel-200 and -201 welded and unwelded corrosion coupons gave low average corrosion rates of ~0.12 mil per day (24 hr) in the halogenation reactor fluid-bed region and <0.09 mil per day above the fluidized-bed region. Even lower corrosion rates of <0.004 mil per day were observed for stainless steel and Inconel coupons in the pyrohydrolysis reactor.

The FBV process, as conceived, appears to offer significant economic advantage over current solvent-extraction reprocessing schemes because (a) small radioactive waste volumes are produced, mostly in solid form; (b) high burnup or short cooled fuels can be reprocessed, without radiation damage to the reagents; (c) overall fewer operations in simple, compact equipment are needed; and (d) the product is uranium hexafluoride, which can be readily used for isotope separation or conversion to the metal or oxide for fuel refabrication.

Two reports, ANL-6829[1] and ANL-6830,[2] summarize the bench-scale development of this FBV process, and a forthcoming report, ANL-6994,[3] summarizes the work with irradiated fuel charges.

I. INTRODUCTION

In nuclear reactors for power generation, several kinds of highly-enriched uranium-alloy fuels are utilized. Uranium-zirconium and uranium-aluminum alloy fuels are most widely used types. For example, highly enriched uranium-zirconium alloy fuels are used in nuclear submarines[4] and in the Shippingport Pressurized Water Reactor (PWR).[5] Uranium-aluminum alloy fuels are commonly used in research and test reactors and in a variety of training reactors such as the Materials Test Reactor (MTR) and the Engineering Test Reactor (ETR). Figure 1 illustrates the size and type of fuels that were processed in the pilot-plant facility.

108-7085C

Fig. 1. Simulated Uranium-Alloy Fuel Elements Used in the FBV Volatility Pilot Plant

Spent forms of the highly enriched uranium-alloy fuels as well as scrap fuel elements require processing to recover the uranium for reuse. Currently, solvent extraction (aqueous) reprocessing methods are being used to recover the enriched uranium.[6] The use of the aqueous reprocessing methods results in large volumes of liquid wastes (which pose storage and handling problems), and radiation damage to the organic solvents is often serious. Minimization, if not elimination, of aqueous, radioactive wastes and the use of reagents that are not susceptible to radiation damage are desirable; fluid-bed fluoride volatility (FBV) techniques appear to offer these advantages.

Other possible advantages of FBV processes include overall fewer operations with relatively simple and compact equipment and direct production of uranium hexafluoride, which can be readily used for isotope separation or conversion to the metal or oxide for reuse as fuel. It appears that fuels decayed for a short time or fuels with very high burnup can be processed by fluoride volatility techniques since the reagents do not suffer radiation damage. These features of the volatility process indicate that considerable economic advantage can be realized in future plants that employ this technique.

A. General Processing Flowsheet

A schematic flowsheet of the FBV process, including provisions for reagent recycle, is shown in Fig. 2. A generalized flowsheet for the FBV processing of enriched alloy fuels, including a discussion of reagent recycle consideration, was presented by Ramaswami et al.[1]

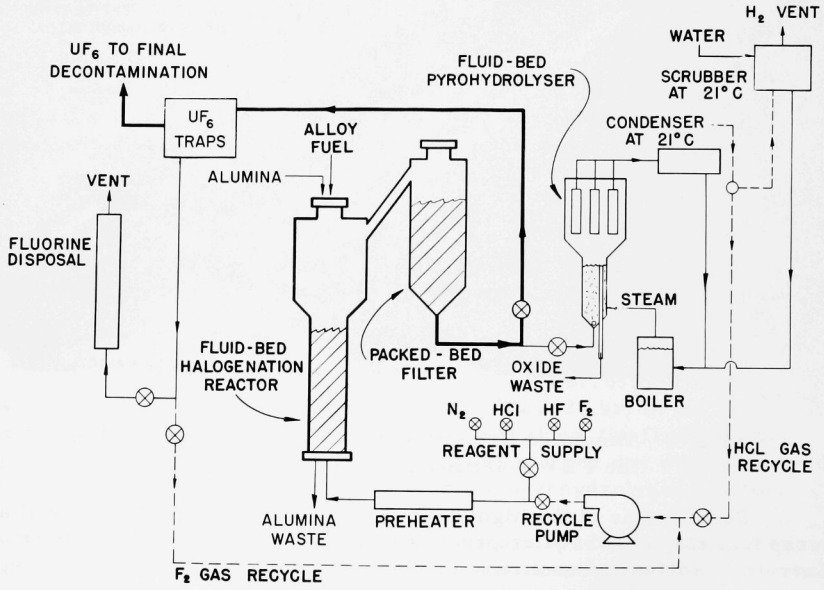

108-8271 Rev. 3

Fig. 2. Schematic FBV Flowsheet for Processing Uranium-Alloy Fuels

The conceptual operation of the FBV process consists of two main chemical reaction steps conducted in a single vessel (halogenation reactor). The first is a separation step, hydrochlorination, in which the alloying

materials are volatilized; the second is a recovery step, fluorination, in which the uranium is volatilized and recovered as the hexafluoride. The reactions are conducted while the fuel is immersed in a bed of inert alumina granules fluidized by nitrogen and reagent gases, which facilitate dissipation of the reaction heat. This flowsheet does not specify details of the final decontamination step since either distillation or sorption-desorption from NaF might be used.[7,8]

In the first step, the alloying elements of the fuel are converted by reaction with HCl into chlorides that are volatile at the reaction temperature. The volatile chlorides of the alloying metal, mainly $ZrCl_4$ in the case of zirconium alloys, and $AlCl_3$ in the case of aluminum alloys, are carried out of the system and are reacted with steam in a second fluid-bed reactor (pyrohydrolysis reactor) to give a solid oxide waste. In the conceptual flowsheet, the HCl regenerated during the pyrohydrolysis operation may be recycled. The uranium forms particulate chlorides, which are relatively nonvolatile and remain in the halogenation reactor system. Any particulate uranium chlorides entrained from the fluid bed by the exiting gas stream are filtered by down-flow of the gas through a static bed of particulate alumina. This type of filter was used because of its simplicity and its suitability with respect to corrosion problems, for high-temperature operation.

In the recovery step, the uranium chlorides in both the halogenation reactor fluid bed and the packed-bed filter are reacted with anhydrous hydrogen fluoride and then gaseous fluorine, and the product (UF_6) is recovered by sorption on beds of NaF at 100°C or in cold traps maintained at about -80°C. The excess hydrogen fluoride and fluorine may be disposed of or may be recycled to the halogenation reactor. The UF_6 may be further decontaminated in a distillation column or by selective sorption on NaF. The decontaminated UF_6 is then returned for isotope separation and reconversion to the metal or oxide for fuel refabrication. The technology of the three final steps, decontamination, isotope separation, and production of highly-enriched uranium-alloy fuel elements, was established previously by others.[4,7,8]

The major amount of the fission-product radioactivity, the nonvolatile fission-product fluorides, will be in a compact form for waste disposal since they will be associated with the particulate alumina from the halogenation reactor and the packed-bed filter. A less active radioactive waste will be the solid oxides produced in the pyrohydrolysis reactor, which will contain the fission products volatilized in the HCl step. Scrub solutions can be vaporized to supply steam to the pyrohydrolysis reactor so that no aqueous wastes will remain. Other nonaqueous wastes may be produced in the product (UF_6) decontamination.

B. Previous Process Development Studies

The FBV process involves volatilization of zirconium or aluminum cladding and alloying material as their chlorides, retention of uranium as relatively nonvolatile chlorides, and subsequent recovery of uranium as the volatile hexafluoride. Three contributions[9,10,11] studied this entire reaction cycle on uranium-Zircaloy-2 (U-Zr) fuels. Some of the individual process steps were studied in connection with the development of other processes.

An exploratory study of processing zirconium fuels, including the hydrochlorination-fluorination reaction cycle, was conducted in a $1\frac{1}{2}$-in.-diam fluid-bed reactor at Brookhaven National Laboratory by Reilly et al.[11] The feasibility of the FBV process was reported. Granular alumina was found to be inert and satisfactory for the fluid-bed material. Uranium recoveries ranged from 93 to 99% of the charge. Use of packed-bed filters for retention of particulate uranium chlorides during hydrochlorination was explored. In addition to the studies in the $1\frac{1}{2}$-in.-diam fluid-bed reactor,[1] a few exploratory experiments were carried out on the hydrochlorination of multiplate uranium-zirconium fuel-element subassemblies in a pilot plant.[12] Satisfactory hydrochlorination rates (~2 kg/hr) were achieved.

Similar attempts at developing the hydrochlorination-fluorination reaction cycle were made in laboratory studies at ANL by Johnson et al.[10] The hydrochlorination and fluorination reactions were conducted in a packed bed of alumina. After the hydrochlorination, the alumina bed was removed and mixed, returned to the reactor, and then fluorinated. The concentration of uranium retained by alumina was low, ranging from 0.007 to 0.043 w/o. These results indicated that high recovery of uranium could be expected.

Simultaneously with the research work at ANL, process development work on a hydrochlorination-fluorination reaction cycle in a fluid bed was being carried out in France for recovering uranium from scrap uranium-zirconium alloy. The results of these development studies, including a semicommercial plant using a 7.9-in.-diam fluid-bed halogenation reactor, were reviewed by Faugeras[9] and Bourgeois et al.[13,14] Residual uranium content of the alumina was ~0.02 w/o. The uranium loss through the packed-bed filter during hydrochlorination was 0.1% of the uranium in the charge. Other workers in France have achieved similar results with aluminum-clad uranium-molybdenum alloys.[15]

The effects of process operating conditions on uranium recoveries were studied intensively by Ramaswami et al.[1,2] at the Argonne National Laboratory. These studies determined optimum fluorination conditions, established high (>99%) uranium recovery, and determined the distribution of the important fission products (simulated with inactive isotopes) and the minor elements of Zircaloy-2,[a] which indicated that a high decontamination factor might be obtained in reprocessing irradiated fuel.

[a] Zircaloy-2 is a high-zirconium alloy, which contains, in addition to zirconium, 1.5% tin, 0.15% iron, 0.10% chromium, and 0.05% nickel.

Other work on the individual process steps and the use of high-temperature packed-bed filter was reviewed by Ramaswami et al.[1,2] The success of the studies of Ramaswami led to the construction and operation of the pilot-plant facility at the Argonne National Laboratory. The details of the pilot-plant phase of the studies on reprocessing uranium alloy fuels are contained in this report. The final phase of this work is currently being conducted wherein irradiated fuels are processed in bench-scale apparatus that is contained in a high-gamma cave facility at ANL. The cave is equipped with master-slave manipulators and is capable of handling about 10,000 Ci of activity.

C. Process Technology

The process under development for the recovery of uranium from alloy fuels employs three principal steps in which chemical separation of the various fuel constituents is achieved by selective volatilization of chlorides and fluorides.

1. Since the concentration of uranium in enriched fuel is low (< 20%), the first step of the reprocessing scheme involves the separation of uranium from the fuel matrix, thereby freeing the uranium for subsequent recovery by fluoride volatility methods. This step is accomplished by reaction of the fuel at about 350°C with hydrogen chloride gas while the fuel is immersed in a fluid bed of inert particles. The hydrochlorination reaction is highly exothermic, giving off 113 kcal/mole, at 298°K, in the case of zirconium, and 100 kcal/mole, at 298°K, in the case of aluminum. Separation occurs through the formation of the volatile chlorides of zirconium and aluminum, $ZrCl_4$ and $AlCl_3$. The $ZrCl_4$ sublimes at 331°C and 1.0 atm; the $AlCl_3$ boils at 180°C and 1.0 atm pressure. Uranium is converted to solid uranium chlorides during the hydrochlorination step and remains, for the most part, associated with the fluid-bed material. However, a portion of the uranium chloride is volatilized and/or entrained in the gas stream; therefore a high-temperature, packed-bed gas filter is employed in series with the fluid-bed reactor to insure adequate retention of uranium within the system.

The volatile metal chlorides ($ZrCl_4$ or $AlCl_3$), produced during hydrochlorination of the metal alloy, represent a waste stream that requires processing for convenient storage. Studies have shown that gaseous $ZrCl_4$ and $AlCl_3$ may be converted directly to solid oxides, ZrO_2 and Al_2O_3, by the gas phase reaction with steam (pyrohydrolysis) in a fluid-bed reactor.[16] This pyrohydrolysis step allows the direct recovery and recycle of the hydrogen chloride reagent.

When the pyrohydrolysis reaction is used to give a metal-oxide product, the reactions of the alloying material are

$$\text{Metal} + HCl \rightarrow \text{Metal-Chloride} + H_2 \qquad (1)$$

and

$$\text{Metal-Chloride} + H_2O \rightarrow \text{Metal-Oxide} + HCl, \qquad (2)$$

giving the net reaction

$$\text{Metal} + H_2O \rightarrow \text{Metal-Oxide} + H_2. \qquad (3)$$

Since this FBV process consumes water, no liquid waste streams need be produced in the hydrochlorination step if the HCl is entirely recycled.

2. In the second step, the uranium chlorides in the fluid-bed reactor and the packed-bed filter are converted to uranium tetrafluoride by reaction with hydrogen fluoride. This step was adopted to reduce the cost of the fluorinating reagent and to avoid the production of gaseous chlorine and chlorine-fluorides in the direct fluorination of uranium trichloride. The presence of these compounds in the reactor off-gas stream would complicate the handling of the UF_6 product since both chlorine and chlorine trifluoride would be condensed with UF_6 in refrigerated traps maintained at about -80°C. Hydrogen fluoride may not be required in the commercial application of the process, especially if the UF_6 product is purified and decontaminated by a selective sorption-desorption procedure using beds of sodium fluoride pellets.[7]

3. In the third step, uranium is recovered as uranium hexafluoride by the reaction between uranium tetrafluoride and fluorine at temperatures of 250 to 500°C. A two-temperature fluorination procedure was developed in the bench-scale studies to assure high recovery of the uranium as uranium hexafluoride.[1,2]

D. Pilot-plant Objectives

The major objectives in the operation of the pilot-plant facility have been to demonstrate (1) complete control of the highly exothermic reactions while processing full-scale alloy fuel elements, (2) the conversion of volatile chlorides of the alloying metal to solid oxides for waste disposal, (3) the operability and efficiency of the packed-bed filter and, (4) the capability of the process for high recovery of the uranium in the fuel.

These demonstration tests were directed toward the recovery of uranium as uranium hexafluoride from unirradiated fuel only. Decontamination of UF_6 from fission-product fluorides can be effected by techniques that have already been developed, such as distillation[8] and sorption-desorption on sodium fluoride beds.[7]

The development work on the hydrochlorination and fluorination of unirradiated, normal uranium-Zircaloy-2 and uranium-aluminum alloys carried out in the pilot-plant facility is summarized in this topical report. The demonstration of a satisfactory reaction cycle for processing enriched alloy fuels is described in terms of the results of the individual reaction steps. The effects of operating variables and equipment design on uranium losses are detailed. This report is based in part on the experimental data, which were reported in the Chemical Engineering Division Summary Reports from Jan 1962 to June 1965 as listed below. A forthcoming topical report by Chilenskas and Turner[3] will summarize small-scale process development work with irradiated fuels.

Report Number	Page	Period Covered
ANL-6543	153	Jan-March 1962
ANL-6569	121	April-June 1962
ANL-6648	172	Oct-Dec 1962
ANL-6687	147	Jan-March 1963
ANL-6725	184	April-June 1963
ANL-6800	282	July-Dec 1963
ANL-6900	194	Jan-June 1964
ANL-6925	149	July-Dec 1964
ANL-7055		Jan-June 1965

II. EQUIPMENT AND INSTRUMENTATION

A pilot plant was constructed to demonstrate the processing of up to 30-kg charges of U-Zr fuel or about 14 kg of U-Al fuel in the form of multiplate assemblies. A schematic diagram of the facility is shown in Fig. 3.

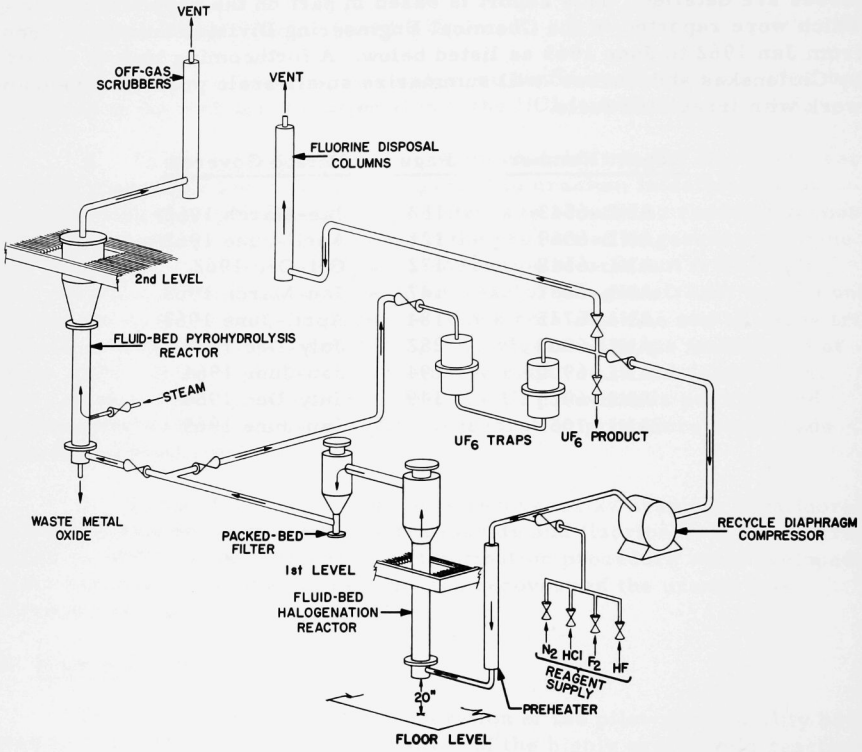

108-7081 Rev. 4

Fig. 3. FBV Pilot Plant for Processing Highly-enriched Uranium-Alloy Fuels

The major equipment items consist of a 6-in.-diam halogenation fluid-bed reactor, a 9-in.-diam packed-bed filter, a 6-in.-diam pyrohydrolysis fluid-bed reactor, two 6-in.-diam uranium hexafluoride product traps, and two 6-in.-diam columns, along with a scrubbing system for disposal of gaseous reagents. A diaphragm pump was also included for possible use in recycling the fluorine and hydrogen chloride process gas streams.

The instrumentation installed in the pilot plant consisted of (1) temperature recorders and an indicator, (2) temperature controllers, (3) pressure and differential pressure transmitters and recorders, (4) flow recorders and controllers, (5) a reactor coolant controller, and (6) thermal-conductivity gas analyzers.

A. Equipment

Details of the equipment size, construction materials, amount of heating, and special features are listed in Table I.

TABLE I. Equipment Specifications

Item of Equipment	Size	Material	Heated or Cooled
Preheater	2-in. ID, 3 ft long	Nickel-200	3 kW
Halogenation Reactor	6-in. Schedule 40 pipe, 70 in. long	Nickel-200	25 kW, air-water cooled
Halogenation Reactor Disengaging Section	12.5-in. ID, 20 in. long	Nickel-200	12 kW
Packed-bed Filter	9.5-in. ID, 27 in. long	Nickel-200	12 kW
Pyrohydrolysis Reactor	6-in. Schedule 40 pipe, 36 in. long	304 stainless steel	16 kW
Pyrohydrolysis Disengaging Section	11.75-in. ID, 28 in. long	304 stainless steel	--
Pyrohydrolysis Filters	2.75-in. OD, 18 in. long	Sintered nickel or Inconel	--
Off-gas Condenser	10.4 sq ft of heat-transfer area	Impervious graphite	water-cooled
Off-gas Scrubber	6-in. ID, 6 ft long	Glass pipe	--
UF_6-NaF Traps	6-in. ID, 21 in. long	Monel	--
F_2 Disposal Columns	6-in. Schedule 40 pipe, 83 in. long	Monel	--
Recycle Pump	25-in.-diam heads, 6-scfm fluorine rated capacity	Nickel process head, 304 SS secondary head	--
Piping: Dry HCl	1- or 1/2-in. Schedule 40 pipe	304 stainless steel	--
F_2	1- or 1/2-in. Schedule 40 pipe	Nickel or Monel	--
Aqueous Waste	1 in.	PVC plastic or Teflon-lined pipe	--

The fluid-bed halogenation reactor is a 6-in.-diam nickel-200 pipe topped with a 20-in. length of 12-in.-diam disengaging section to make an overall reactor length of 8 ft 5 in. The heaters and cooling coils were brazed in place on the reactor before a 1/8-in.-thick spray coating of copper was applied for better heat transfer to the reactor walls (Fig. 4). A thin overspray of stainless steel was applied for oxidation protection. The heated gas from an internally-finned preheater enters the reactor through a bubble-cap gas distributor, which is attached to the bottom of the reactor. After installation, the reactor and the other process components were covered with approximately 2 in. of insulation.

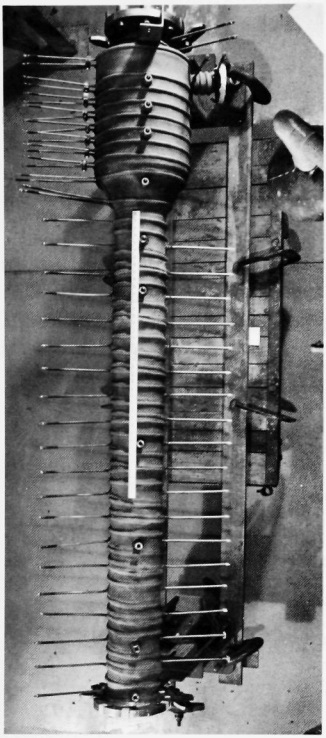

108-5549

Fig. 4. Fluid-bed Halogenation Reactor before Installation

The packed-bed filter is a 9.5-in.-diam, internally-finned pipe, which tapers to a 1.5-in. diam at the bottom, to make an overall length of 27 in.

The pyrohydrolysis reactor (Fig. 5) is a 6-in.-diam, 36-in.-long, 304 stainless-steel pipe, topped by a 11.75-in.-diam, 28-in.-long disengaging section containing sintered Inconel or nickel filters (18 in. long, $2\frac{3}{4}$ in. diam), which are periodically cleaned in place with a blowback of preheated nitrogen. Each filter is blown back every 1.5 min. The process stream from the packed-bed filter enters the pyrohydrolysis reactor through a 60° cone bottom, which has a ball-check valve for retaining solids. An overflow pipe is connected to a product pot, located under the pyrohydrolysis reactor, and extends inside the reactor to a height of 21 in. The overflow pipe and product pot are maintained at temperatures above the condensing point of steam. The product flows from the top of the fluid bed via the overflow pipe to the product pot by gravity feed.

The uranium hexafluoride traps consist of two series-connected Monel containers, 21 in. high by 6-in. diam. The UF_6 product is collected by sorption on two beds, each containing about 7 kg of sodium fluoride pellets.

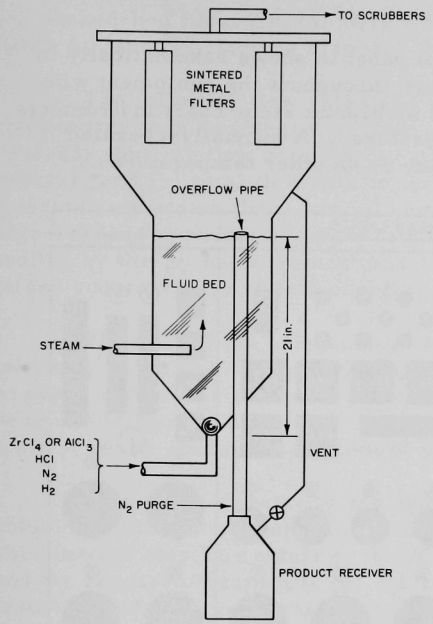

108-7981 Rev.

Fig. 5. Fluid-bed Pyrohydrolysis Reactor

The HCl off-gas disposal system consists of an impervious graphite condenser followed by a scrubber, which uses recirculating water. Sufficient steam is added to the HCl-H_2O off-gas from the pyrohydrolyzer so that the resulting liquid, condensed at about 20°C, contains about 5 N HCl. The off-gas from this condensate (mainly nitrogen from purges and diluent gas) is passed through the scrubber for final HCl removal. The excess fluorine is disposed of in 6-in.-diam Monel columns, which contain 6-ft-deep beds of coarse (1/4- to 1/2-in.) activated alumina.

Power for heating is supplied by a two-wire, 240-V system through twelve 10-Amp and seven 25-Amp variable-voltage transformers. Each of the larger transformers operates in conjunction with a proportioning-type temperature controller.

The valves used for dry HCl are bellows-sealed and constructed of stainless steel. The valves used for fluorine are constructed of Monel and are sealed by Monel bellows. Two all-nickel, double-bellows-sealed valves are used in the high-temperature region just downstream of the packed-bed filter.

Spiral-wound gaskets of a nickel-asbestos combination are used in the primary reactor and packed-bed filter, with the exception of the charge ports on both vessels, where serrated gaskets of solid, annealed nickel are used. Spiral-wound gaskets of stainless steel-asbestos are used in the pyrohydrolysis reactor.

The process piping is nickel or Monel for the fluorine and hydrogen fluoride streams. Type 304 stainless steel is used for the dry hydrogen chloride supply and for the HCl-steam mixture at temperatures above the dew point. Plastic and glass equipment are used to handle the condensed HCl-H_2O.

The heat produced during the exothermic hydrochlorination reaction is removed from the fluid-bed section of the halogenation reactor by an air-water mixture, which is passed through stainless-steel coils in four cooling zones.

B. Instrumentation

The instrumentation and control panel is shown schematically in Fig. 6. The temperatures are monitored throughout the equipment with Chromel-Alumel thermocouples. Two multipoint strip-chart instruments record 36 of the most important temperatures. A manually-operated temperature indicator monitors as many as 48 other temperatures.

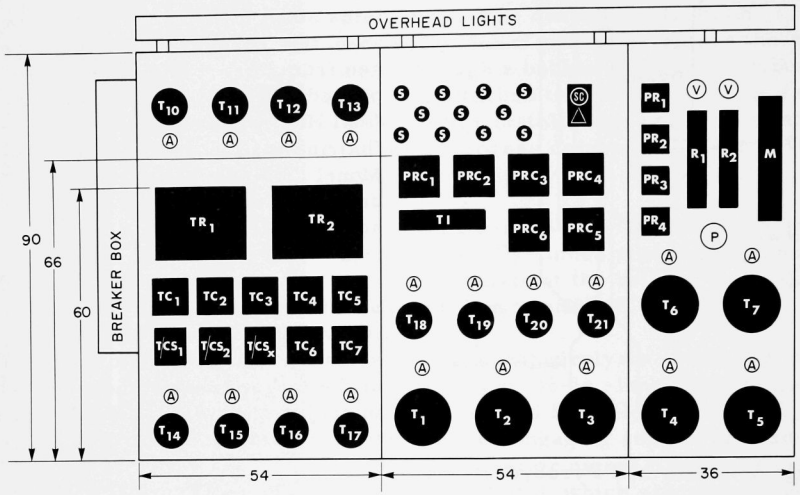

Fig. 6. Pilot-plant Instrumentation Panel

Proportioning-type temperature controllers regulate the electrical power to the equipment heaters. The heaters are wired so that several of them may be used for a particular zone. Two heated zones are controlled on the halogenation reactor, one on the halogenation-reactor disengaging section, one on the packed-bed filter, two on the pyrohydrolysis reactor, and one on the gas preheater. The controller for each zone operates by means of a signal from a thermocouple in contact with the walls of the respective vessels.

The following pressures and differential pressures (Δp) are measured by pneumatic transmitters and recorded on 4-in. strip-chart recorders: (1) primary reactor bed Δp, (2) total system pressure,

(3) packed-bed filter Δp, (4) pyrohydrolyzer bed Δp, (5) pyrohydrolyzer filter Δp, and (6) fluorine disposal column Δp.

The following flow rates are recorded by using a pneumatic Δp transmitter with an integral orifice: (1) nitrogen flow rate, (2) HCl flow rate, (3) fluorine flow rate, (4) steam flow rate for the pyrohydrolysis reactor, and (5) total flow rate to the halogenation reactor. The HCl, fluorine, and steam flows are all controlled by pneumatic valves using the signal from the respective flow orifices. The nitrogen flow rate is controlled by the Δp measurement of total flow so that the total flow rate is maintained constant to provide a constant fluidizing velocity.

The wall of the halogenation reactor is cooled by an air-water mixture, which is circulated through a series of four stainless-steel coils wrapped around the reactor. A thermocouple attached to the wall is the sensing element. The flow of coolant is regulated by a temperature controller, which operates a system of pneumatic valves.

Thermal-conductivity gas analyzers are used to follow the hydrochlorination and fluorination steps of the reaction. During the hydrochlorination step, the extent of the HCl reaction, the metal reaction rate, and the required steam rate for the hydrolysis reactor are determined from the hydrogen production rate. The concentration of hydrogen produced during the alloy reaction is measured by comparing the thermal conductivity of a sample of the off-gas (a mixture of hydrogen and nitrogen) from the final scrubber with that of a reference gas (pure nitrogen). The thermal-conductivity cell can be easily calibrated with known mixtures of hydrogen and nitrogen and, therefore, provides accurate, quantitative information. The extent of the fluorination reaction is followed qualitatively by comparing the thermal conductivity of nitrogen to that of the fluorine-nitrogen-UF_6 mixture that enters the NaF traps. These systems are discussed in more detail in Appendix C.

III. OPERATING PROCEDURE AND CONDITIONS

The experimental procedure includes bed preparation, prefluorination, fuel charging, hydrochlorination, hydrofluorination, fluorination, and sampling.

A. Bed Preparation

A predetermined quantity of particulate material (sintered or fused alumina) is charged to the halogenation reactor, packed-bed filter, and pyrohydrolysis reactor. The settled halogenation-reactor bed depth is about 48 in., the packed-bed filter depth is 5 to 12 in., and the settled pyrohydrolysis-reactor bed depth is about 21 in.

The two uranium hexafluoride traps are filled with NaF·HF. These traps are heated to 350°C to drive off the HF and leave the NaF, which is later used to adsorb the UF_6 product. The excess HF from the traps is reacted with soda lime in one of the off-gas disposal columns.

B. Prefluorination

The purpose of the prefluorination step is to form a layer of nickel fluoride, which decreases the extent of corrosion of inner surfaces of the equipment during the hydrochlorination and hydrofluorination steps. Only one initial prefluorination should be necessary in a plant that is operated continuously, since the protective layer would not be subjected to the destructive influence of thermal cycling.

The prefluorination procedure consists of setting the fluorine flow rate at 0.1 cfm and the nitrogen flow rate at 4.0 cfm, with the process equipment at a temperature of 250°C. The equipment is then heated, and at 500°C the nitrogen flow is stopped and the fluorine flow is maintained at 0.1 cfm for 2 hr before being turned off. Usually a total time of 5 hr is required for the prefluorination step. The pyrohydrolysis reactor does not receive the prefluorination treatment.

C. Fuel Charging

The fuel element is placed on the settled halogenation reactor bed (Fig. 7) and then lowered slowly to the bottom of the bed by admitting, intermittently, pulses of nitrogen gas.[18] A remotely-operated device to lower the fuel onto the settled bed would be required for irradiated fuels.

D. Hydrochlorination

The entire reaction system is heated to the desired temperature while sufficient nitrogen is passed through the equipment to fluidize the

alumina in the halogenation reactor and the pyrohydrolysis reactor. The gases entering the halogenation reactor are heated to 350°C in the preheater. Steam is admitted to the pyrohydrolysis reactor shortly before the flow of HCl is started to the halogenation reactor. The volatile chlorides produced during hydrochlorination are converted to oxides by reaction with steam in the fluid-bed pyrohydrolysis reactor at about 350°C. The product from the pyrohydrolysis reactor is continuously withdrawn through an overflow pipe.

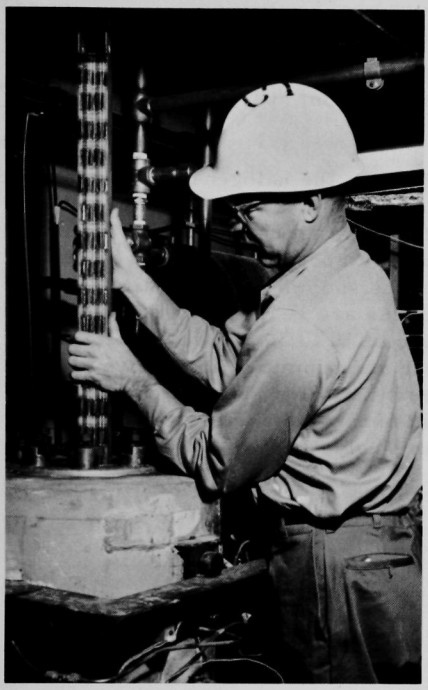

108-6562

Fig. 7. Charging Fuel to the Halogenation Reactor

The halogenation reactor wall-cooling system, in which the coolant is an air-water mixture, maintains the reactor wall at the preset controller temperature of 350°C. The hydrochlorination reaction is allowed to proceed until the thermal-conductivity analyzer shows that the hydrogen production has ceased.

E. Hydrofluorination

After the flow of HCl is shut off, the temperature is adjusted to that desired for the hydrofluorination step (350°C). The off-gas from the packed-bed filter is routed so that it will bypass the pyrohydrolysis reactor into a bed of soda-lime for HF disposal, and then HF is fed at the desired rate of 20-25 g/min for 1 to 2 hr. The system is purged, and the temperature is adjusted to the desired fluorination condition.

F. Fluorination

The fluorination is started, with the halogenation reactor and packed-bed filter at 250°C, using 1 to 5 v/o fluorine in nitrogen. The temperature is then raised to 500°C, at which point the nitrogen dilution is reduced so that the reactor bed is no longer fluidized and the fluorine concentration is 30 to 80 v/o in nitrogen. The total fluorination time required is 4 to 9.5 hr. Two sodium fluoride beds are maintained at about 100°C for sorption of the product UF_6.

G. Sampling

Concurrent with the operation of the experiment, the halogenation reactor bed is sampled. A 1/4-in. ball valve, located on the side of this reactor, approximately 30 in. from the reactor bottom, is used to obtain samples while the bed is fluidized. Samples are obtained from this valve at scheduled times during the hydrochlorination, hydrofluorination, and fluorination steps.

At the end of each run, the beds from the halogenation reactor, the packed-bed filter, pyrohydrolysis reactor, sodium fluoride trap, and fluorine disposal tower are removed from the process vessel, weighed, and passed through a sample size reducer to obtain a sample weighing about 1/16 of the original bed weight. The sodium fluoride pellets are ground to -8 mesh. All of the bed samples are reduced in size with a sample splitter (1:1) until a sample size of 10 to 30 g is obtained. These small samples are ground to -200 mesh and submitted for analysis. The sample from the fluorine disposal tower (activated alumina) is weighed and leached with 10% nitric acid a total of three times. A sample of the leach solution is submitted for uranium analysis.

IV. RESULTS AND DISCUSSION

A total of 18 experiments were completed in the pilot-plant facility. The initial six runs (three Zircaloy and three aluminum assemblies) involved processing of simulated fuel charges that did not contain uranium. These runs were used to test the equipment and instrumentation and to establish procedures and conditions for the later runs with uranium alloys. The fluorination step was not performed in these six runs because of the absence of uranium. The last 12 runs were made with uranium alloy fuels (four with U-Zr fuel and eight with U-Al fuel). All the runs were operationally successful.

The typical conditions and results from processing batch charges of either zirconium or aluminum fuel are summarized in Table II. These data

TABLE II. Typical Processing Conditions and Observed Results for Pilot-plant Experiments

	Uranium-Zircaloy-2 Fuel, PWR Type	Uranium-Aluminum Fuel, MTR and ETR Types
I. Hydrochlorination		
A. Typical Charge		
Weight (kg)	20	7
No. of Plates	14	19
Length (in.)	48	36
Uranium (g)	180	280
B. Average HCl Gas Inlet Concentration (v/o)[a]	80	80
C. Fluidization Velocity (ft/sec)	0.4-0.6	0.4-0.6
D. Process Temperature (°C)		
Halogenation Reactor Bed	450	350
Halogenation Reactor Wall	350	300
Packed-bed Filter	350	200
Pyrohydrolysis Reactor	350	350
E. Observed Results		
Reaction Rate (kg/hr)	2.0-3.0	0.9-1.5
Average HCl Utilization (%)	25-35	45-50
F. Reaction Time (hr)	7-10	4-6
II. Hydrofluorination		
A. HF Gas Inlet Concentration (v/o)[a]	10-20	
B. Fluidization Gas Velocity (ft/sec)	0.5	
C. Process Temperature (°C)		
Halogenation Reactor Bed	350	
Packed-bed Filter	350	
D. Reaction Time (hr)	1.0-2.0	
III. Fluorination		
A. F_2 Gas Inlet Concentration (v/o)[a]		
Initial Period	1-5	
Final Period	30-80	
B. Gas Velocity (ft/sec)		
Initial Period (fluidized bed)	0.5	
Final Period (settled bed)	0.03	
C. Process Temperature (°C) Halogenation Reactor Bed and Packed-bed Filter		
Initial Period	250 increasing to 500	
Final Period	500	
D. Reaction Time (hr)	4-9.5	

[a]Nitrogen diluent.

are not necessarily optimum but represent the processing conditions that resulted in satisfactory operation and uranium recovery. The conditions and results for each run are presented in Appendix A.

A. Hydrochlorination

Both U-Zr and U-Al fuels were hydrochlorinated in the fluid-bed halogenation reactor by using inlet-gas streams containing 60 to 98 v/o HCl in nitrogen. The operating characteristics of this step were similar for both fuels, except that the relative low density of the U-Al fuel elements required that they be mechanically submerged in the fluid bed since they had a tendency to float on top of the fluid bed. In all runs, the cooling system controlled the reaction by maintaining the bed temperatures at 350-400°C. The maximum fuel-plate temperatures were 700°C for the U-Zr fuels and 570°C for the U-Al fuels. Both are well below the melting points of the respective alloys.

Inspection of partially-hydrochlorinated charges showed that the fuel reacted more rapidly near the bottom of the reactor, in the vicinity of the reagent gas inlet. A partially-hydrochlorinated (~80%) U-Zr fuel element and a similar unreacted fuel element are shown in Fig. 8. The part of the reacted fuel element on the left side of the figure was pointed down in the reactor. The U-Al fuel elements reacted in a similar manner, but the plates did not become separated since they are held together by 1/4-in.-thick side plates, which require more time for complete reaction than do the thinner (U-Al) fuel plates (about 0.055 in. thick).

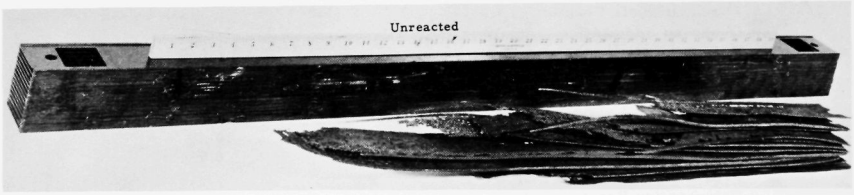

108-8004

Fig. 8. Effect of Hydrochlorination on a U-Zr Simulated Fuel Subassembly

The average alloy reaction rate for batch charges of U-Al fuels has been in the range 0.9 to 1.5 kg/hr, which results in a time of about 5.5 to 7.0 hr for complete hydrochlorination of one fuel element. Maximum rates of 3.0 kg/hr have been achieved during the initial period of hydrochlorination. The average alloy reaction rates for batch charges of U-Zr fuel were about 1.8 kg/hr for a 14-plate subassembly and about 1.4 kg/hr for a nine-plate subassembly. For both sizes of elements, the maximum alloy reaction rates were about 3.3 kg/hr during early portions of the runs.

Comparison of the reaction-rate data for individual runs indicated that higher reaction rates could be achieved by using a superficial fluidization velocity of 0.6 ft/sec compared to the results at 0.4 ft/sec. There was no significant decrease in the HCl utilization at the higher velocity. The reaction rate was also related to the amount of the fluid-bed cross section that was occupied by fuel plates. That is, more plates per fuel element gave higher reaction rates because more of the HCl was able to pass through, rather than around, the fuel element. Longer fuel elements also react faster than short elements, but since the reaction is localized primarily at the bottom of the reactor, the effect of length is less important than is charging the halogenation reactor, so that the fuel elements efficiently fill the cross section of the bed.

The percentage of the inlet HCl consumed in the reaction on a single pass has been relatively high in batch-processing runs. Average utilizations of about 40% have been achieved for the aluminum fuels and about 25% for zirconium fuels. Over 80% of the inlet HCl was utilized in the early portions of runs with both fuel types.

The HCl inlet concentration, reaction rate, and HCl utilization for a typical run with U-Al fuel (Run 8) are plotted as a function of time in Fig. 9 for a batch charge of fuel. These data were calculated and plotted by using digital-computer techniques as described by Holmes and

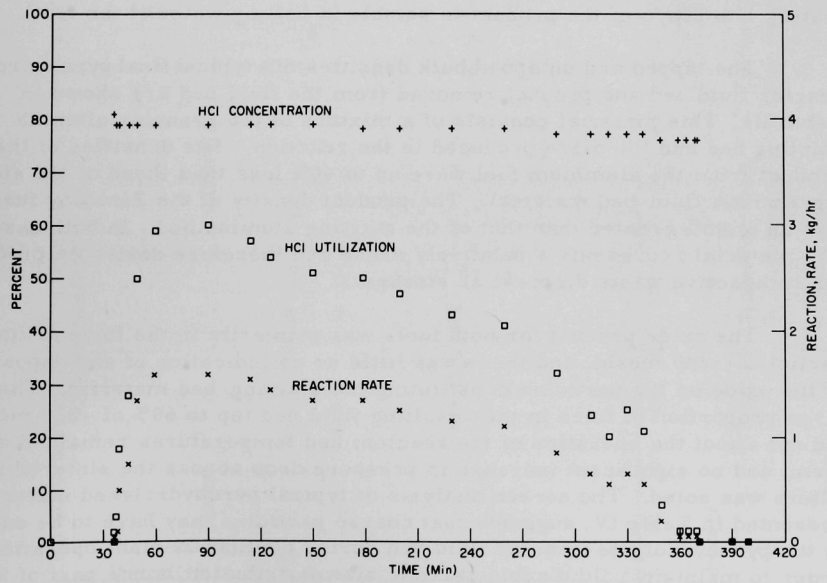

108-8117 Rev. 2

Fig. 9. Reaction Rate, HCl Utilization, and Input HCl Concentration as a Function of Time for Processing One U-Al Fuel Charge

Ramaswami.[17] The reaction rate and efficiency are relatively constant during the first half of the run (constant-rate period); they decrease slowly (falling-rate period) in the later part of the run. Experiments in which an additional fuel element was charged after 60 to 80% of the previous one had reacted (a total of three elements were used) showed an increase in both the average reaction rate and HCl utilization by about 25% over the values achieved in similar single-element experiments. That is, using the multiple-charge technique with three fuel charges, the average utilization was increased to about 50% and the reaction time per element was reduced to about 4-5 hr for the U-Al fuels. The HCl inlet concentration, reaction rate, and HCl utilization are shown for a multicharge run with U-Al fuel (Run 10) in Fig. 10. Similar improvements were also achieved with U-Zr fuels by means of the multicharge technique.

The pyrohydrolysis reactor for converting the zirconium and aluminum chlorides to their respective solid oxides operated smoothly in all experiments. The rate of addition of steam to the pyrohydrolysis reactor was such that the total quantity of water was three times the stoichiometric requirement for the conversion of chloride to oxide. Chemical analyses of the solid products indicated that the residual chloride content ranged from 0.3 to 3.0 w/o in the U-Zr runs and 4 to 10 w/o in the U-Al runs. This quantity of chlorides in the waste oxide (probably present as oxychlorides) is not expected to be harmful to the storage properties of the solid. Approximately 1 to 2 w/o of the product is soluble in boiling water (1-hr test).

The tapped and untapped bulk densities of a typical final pyrohydrolysis-reactor fluid bed and product removed from the fluid bed are shown in Table III. This material consists of a mixture of the granular alumina starting bed and the oxide produced in the reaction. The densities of the product from the aluminum fuel were up to 40% less than those of the starting alumina fluid-bed material. The product density of the Zircaloy fuels was up to 40% greater than that of the starting alumina bed. In both cases, this material represents a relatively dense and therefore desirable product for radioactive waste disposal or storage.

The oxide product for both fuels was primarily in the form of fine particles (-200 mesh), and there was little or no indication of any deposition of the oxide on the particles constituting the starting-bed material. The large proportion of fines in the resulting fluid bed (up to 60% of -230 mesh) did not affect the operation of the reactor; bed temperatures remained uniform, and no significant increase in pressure drop across the sintered metal filters was noted. The screen analysis of typical pyrohydrolyzed material, presented in Table IV, suggests that coarse particles may have to be added to the pyrohydrolysis-reactor fluid bed during continuous plant operation in order to maintain a fluidizable particle size distribution, since part of the coarse bed is removed continuously with the product.

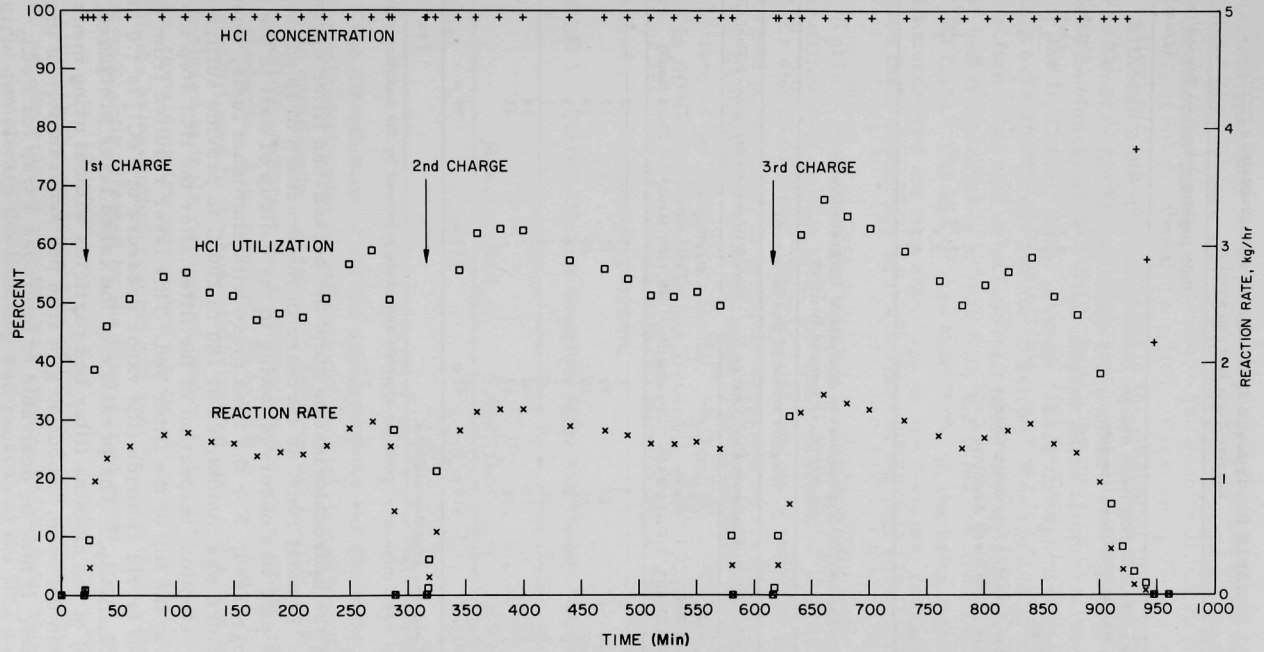

108-8116 Rev. 2

Fig. 10. Reaction Rate, HCl Utilization, and Input HCl Concentration as a Function of Time for Processing Three U-Al Fuel Charges

TABLE III. Typical Bulk Density of Pyrohydrolysis-reactor Fluid Bed and Product

	Bulk Density (g/cm^3)	Tapped Density (g/cm^3)
Uranium-Aluminum Fuel, 6.0-kg Batch Charge 10.0-kg Starting Bed 48-100 Mesh Alumina		
Starting Bed	1.62	1.86
Product	1.1	1.5
Final Fluid Bed	1.8	2.1
Uranium-Zircaloy-2 Fuel, 13-kg Batch Charge 10-kg Starting Bed 28-48 Mesh Alumina		
Starting Bed	1.75	1.90
Product	2.3	2.7
Final Fluid Bed	1.7	2.4

TABLE IV. Typical Screen Analysis of Pyrohydrolysis-reactor Fluid Bed and Product

	Weight Percent of Bed on Screen					
	Batch Uranium-Aluminum Fuel Charge			Batch Uranium-Zircaloy-2 Fuel Charge		
Screen Size	Starting Fluid Bed -48 +100 Mesh[a]	Final Fluid Bed[b]	Product[b]	Starting Fluid Bed -48 +100 Mesh[a]	Final Fluid Bed[b]	Product[b]
+60	5	3	2	5	2	2
+80	47	23	19	47	17	13
+120	40	25	20	40	18	14
+170	6	4	2	6	3	2
+230	1	1	3	1	1	1
+325	1	10	12	1	14	16
-325	-	34	42	-	45	52
Average Size	183 μ	114 μ	97 μ	183 μ	91 μ	78 μ

[a]The starting fluid bed was granular alumina.

[b]The final material was a mixture of granular alumina and oxide produced by the reaction with steam.

During the hydrochlorination step, the packed-bed filter operated satisfactorily. In most runs, an increase in the pressure drop across the filter of 2 to 4 psig was observed, owing to the buildup of dust in the filter as the run progressed. For the runs made with aluminum fuels, when the filter temperature was maintained at 180 to 200°C to provide sufficiently high uranium retention, inspection of the filter after the HCl step revealed a caked layer at the top of the filter bed. This layer resulted from the condensation of ferric chloride (the vapor pressure of $FeCl_3$ is 1.0 atm at 319°C) or $FeCl_3$-$AlCl_3$.[19] The presence of the caked layer precluded the ready removal of the alumina filter bed particles without using mechanical means to loosen the cake. About 40 g of iron per subassembly is present in the U-Al fuel. It may be desirable to interpose a trap for $FeCl_3$

condensation upstream of the filter bed, since the presence of iron chloride also caused temperature excursions at the surface of the packed-bed filter during the fluorination step.

Although some iron is present in the U-Zr fuels, no filter-bed caking occurred because the higher filter temperature (350°C) used in these runs prevented condensation of $FeCl_3$. Higher filter temperatures cannot be used for the U-Al fuel, since uranium losses through the filter become appreciable over 200°C (see Section D below). Ramaswami et al.[2] reported high reaction rates and no packed-bed filter caking when using halogenation reactor bed temperatures of less than 300°C for the hydrochlorination step with U-Al fuels. The use of less than 300°C in the halogenation reactor apparently condensed the iron chlorides on the fluid-bed particles and thus prevented their deposition on the surface of the packed-bed filter.

Table V shows how the uranium was distributed in the halogenation reactor-filter system just after the hydrochlorination step of typical runs with U-Zr and U-Al fuels. The uranium, which is reported as not associated with the bed particulate, is probably deposited on the walls of the reactor above the fluidized bed or in the form of nonfluidizable particulate material at the bottom of the fluid-bed reactor. Holding the U-Al fuel elements submerged in the fluidized bed did not alter this distribution. The low percentage of uranium associated with the reactor bed in the case of the U-Al fuel caused no operational problems.

TABLE V. Distribution of Uranium after the Hydrochlorination Step

	U in Reactor Bed	U in Filter Bed	U Not Associated with the Beds
U-Al Fuel	~20%	~15%	~65%
U-Zr Fuel	~70%	~15%	~15%

The distribution of the tin and iron from the Zircaloy-2 fuel charges was determined in order to indicate the path of fission products having similar volatile compounds. These data confirm the results of Ramaswami et al.[1] who, in addition, reported the distribution of several compounds of fission-product elements. Approximately 90 to 98% of the tin and 20 to 30% of the iron are volatilized in the hydrochlorination step. The iron and tin are then pyrohydrolyzed to their respective oxides along with the bulk of the zirconium. The remaining few percent of tin and 70 to 80% of the iron are associated with the halogenation-reactor bed and the filter bed. This distribution is not significantly affected by the fluorination step.

Although the concentration of fluoride ion in the HCl-stream off-gas from the pyrohydrolysis reactor was expected to be low, high concentrations might complicate the handling and recycle of the HCl due to corrosion

consideration. The average fluoride concentration of the HCl-stream condensate from the pyrohydrolysis reactor was 0.03 g/liter, which is probably sufficiently low to permit the use of standard HCl recycle equipment and techniques.

Several generalizations were made concerning the operational characteristics of the hydrochlorination step when processing U-Zr or U-Al fuels:

1. The reaction rate was nearly independent of bed temperature in the range of 330 to 400°C during the initial part of the run when the HCl utilization is high.

2. Gas velocities in the fluid-bed halogenation reactor of about 0.6 ft/sec gave higher reaction rates with little or no decrease in HCl utilization efficiency than did velocities of about 0.4 ft/sec.

3. A satisfactory combination of high reaction rate along with high HCl utilization can be achieved by using about 80 v/o HCl in nitrogen as the feed gas to the reactor.

4. An increase in the overall HCl utilization efficiency and reaction rate can be realized by charging additional fuel after the previous charge has reacted to a point where the rate and utilization of HCl begin to decrease. This procedure may be important in reducing the total processing time and may increase the through-put capacity of the process equipment.

5. The packed-bed filter operated satisfactorily, even though a surface cake was formed during the hydrochlorination step of the runs with aluminum fuel. Means of avoiding the caked layer by minor design or operating changes appear to be readily available.

6. The pyrohydrolysis reactor, located in series with the halogenation reactor and the packed-bed filter, operated satisfactorily.

B. Hydrofluorination

The hydrofluorination step was conducted to convert the uranium chlorides to their respective fluorides in order to minimize the formation and subsequent handling of chlorine-fluorine compounds in the fluorination step. Typical operating conditions and results were presented in Table II.

The residual chloride content of the reactor bed after the HF treatment was 0.004 to 0.01 w/o, which corresponds to about 2 to 6 g of chlorine in the entire reactor and filter system. Figure 11 illustrates that the

minimum residual chloride value can be obtained in about 45 min, which confirms the data presented by Ramaswami et al.[1] Further hydrofluorination is therefore unnecessary.

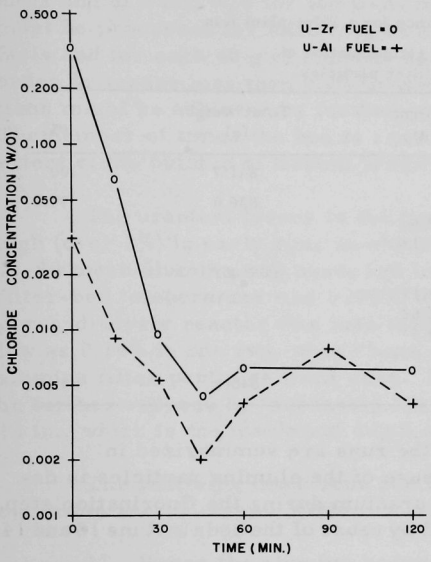

108-8401

Fig. 11. Chloride Concentration of the Halogenation-reactor Bed during Hydrofluorination

C. Fluorination

The fluorination step of all the runs was performed without using the fluorine recycle. The operating conditions and results were presented in Table II. The overall fluorine requirement was about 8 g of fluorine per gram of uranium recovered, and as little as 2.7 g/g were required in one run. This implies that the reagent cost of fluorine would be as low as a few cents per gram of uranium. Since the fluorine requirements are quite low, a fluorine recycle procedure may not be required for plant-scale operation.

The fluorination step of each run with U-Zr fuel proceeded without difficulty. The time required to complete the fluorination ranged from 4.0 to 8.3 hr. During the fluorination step of the U-Al alloy runs, temperature excursions were encountered at the caked surface of the packed-bed filter when the fluorine concentration was increased from about 2 to about 50%. These temperature excursions were related to the deposition of iron chloride, as described previously, and were minimized in subsequent runs by conducting the fluorination at a slower rate. These excursions can probably best be eliminated by preventing the deposition of iron chlorides on the filter bed, as discussed previously, or by providing means to fluidize the filter bed during fluorination so that the heat of reaction can easily be removed. Even though the halogenation reactor bed was not fluidized during the final fluorination period, no caking or temperature excursions were encountered for either type of fuel.

D. Uranium Disposition and Material Balance

The demonstration of recoveries of over 99% of the uranium in the fuel charge as UF_6 was of prime importance in the overall pilot-plant program. Table VI gives the uranium material balance for a run in which over 99% of the uranium was recoverable and 99.9% was accounted for. The

recovery demonstrated in this run is considered typical of what can be readily achieved in this process. The uranium material balances are summarized in Appendix A.

TABLE VI. Uranium Balance for a Pilot-plant Run

(Run 9; including refluorination of the packed-bed filter particles)

	Weight (g)	Total Weight (g)	(%)
Total Uranium Charge		841.7	100
U Recoverable		836.0	99.3
In UF_6 trapping system	832.9		
In bed samples	3.13		
U Lost		4.7	0.6
To pyrohydrolysis reactor	3.17		
To halogenation reactor bed	0.62		
To filter bed	0.9		
To scrub system	0.001		
U Accounted For		840.7	99.9

The uranium loss data for all the runs are summarized in Table VII. These data indicate that reuse of the alumina particles is desirable in order to reduce the loss of uranium during the fluorination step. A two-fold improvement was achieved by reuse of the beds in Runs 13 and 14

TABLE VII. Summary of Uranium Loss Data

Run No.	U Charge	Pyrohydrolysis Reactor (g)	Pyrohydrolysis Reactor (%)	Halogenation Reactor Bed (g)	Halogenation Reactor Bed (%)	Packed-bed Filter (g)	Packed-bed Filter (%)	Final U Concentration of Reactor and Filter
				Uranium-Zircaloy-2				
7	182 ± 4	4.7[d]	2.6	1.4	0.8	0.9	0.5	0.01 w/o U
13	117 ± 4	0.3	0.2	5.7[r]	1.9	1.5	1.3	
14	~160	0.25	0.2	3.8[r]	0.8	1.6[r]	0.4	
15	546 ± 10	4.4	0.8	4.3	0.8	2.9	0.5	
				Uranium-Aluminum				
8	273.6	8.6[t,d]	3.1	0.35	0.13	2.1	0.2	0.005 w/o U
9	841.7	3.2	0.4	0.62[r]	0.06			
10	828.2	4.4	0.5	5.2[r]	0.3	3.5[c]	0.4	
11	280.4	1.9	0.7	*	*	*	*	
12	285.7	0.13	0.05	2.3[r]	0.10	0.4[c]	0.14	
16	275.9	18.0[t]	6.6	3.3[r]	0.12	1.1	0.4	
17	292.3	4.9[t]	1.7	3.5[r]	0.11	0.9	0.31	
18	283.5	4.2[t]	1.5	0.9[r]	0.03	4.2[c]	1.5	

[r]Bed particulate reused from the previous run; % is based on U charged in this run and all prior runs.

[t]Filter-bed temperature too high, causing high U losses.

[d]Filter-bed depth insufficient during HCl step, causing high U losses.

[c]Caking at surface of the packed-bed filter; retention can be reduced by fluroination as a fluidized bed.

*No fluorination step conducted.

with the U-Zr fuel. The loss to the halogenation-reactor bed was only 0.03% in the series of seven runs (8, 9, 10, 12, 16, 17, and 18) with U-Al fuel. The final uranium concentration in the bed of 0.01 w/o for U-Zr fuels and of 0.005 w/o for the U-Al fuels indicate that 1.0 g of uranium must be processed for each 20 g of alumina bed in the case of the U-Zr fuels and for each 40 g of alumina bed in the case of the U-Al fuels in order to assure less than 0.2% uranium loss. Lower uranium concentrations might be achieved by further optimizing the fluorinating conditions. The number of times the bed is reused will probably be limited by the extent of the buildup of fission products that generate heat.

The uranium losses to the pyrohydrolysis reactor were relatively high (over 2%) in early runs in which a filter-bed depth of 4 to 8 in. of 14-28 mesh alumina was used, and in runs with the U-Al fuel in which the filter-bed temperature was >200°C during the HCl step. The loss to the pyrohydrolysis reactor was less than 0.8% in the remaining runs, and as low as 0.14% in one run, where beds 11 to 12 in. deep, of 14-48 mesh alumina filter particles were used. It is expected that these losses could be further reduced by increasing the filter-bed depth[1] to greater than 12 in., which is the maximum depth available in the existing equipment.

The following conditions and techniques are recommended for smooth operation and to assure >99% uranium recovery:

1) Reuse the alumina bed material for a number of reaction cycles.

2) Provide a means of efficient cooling of the packed-bed filter to minimize possible temperature excursions during the fluorination step. Fluidization would provide satisfactory cooling.

3) Use the two-temperature (250-500°C) fluorination procedure that was developed by Ramaswami *et al.*[1] and again detailed in Section III of this report.

4) Employ a packed-bed filter depth of over 12 in. and a filter temperature of 180-200°C for the U-Al fuels, and 335-350°C for the U-Zr fuels.

V. OVERALL PROCESS CONSIDERATIONS

A. The Degradation of Alumina

The attrition of Type T-61 Alcoa alumina was measured for all runs. On an average, ~1.0% of the halogenation-reactor bed per run was attrited so that this amount (~0.4 kg) was entrained by the gas stream and deposited on the packed-bed filter. The same reactor-bed particulate material was reused in a series of seven complete reaction cycles without any apparent change in the attrition rate per run. The initial and final screen analysis of the reactor bed for the seven reaction cycles is shown in Table VIII. Although there was a larger percentage of fine particles, the average particle size changed by only 8%, ~260 to ~240 microns. This amount of degradation did not measurably affect the fluidization or heat-transfer properties of this bed material.

TABLE VIII. Screen Analysis of the Halogenation-reactor Bed

U. S. Screen Size	Starting T-61 Alumina Nominal 28-100 Mesh (w/o)	T-61 Alumina after Seven Complete Reaction Cycles (w/o)
+45	21	23
+60	27	30
+80	25	20
+120	22.5	20
+170	3.5	5.5
+230	0.5	1.5
+325	0.5	1.0
-325	-	-
Average Size	~260 microns	~240 microns

B. Corrosion

Nickel-200 and -201 welded and unwelded corrosion coupons in the halogenation reactor gave corrosion rates ranging from 0.08 to 0.12 mil per day (24 hr) in the fluidized-bed region and 0.03 to 0.09 mil per day above the fluidized bed. The data were taken from defilmed coupons and calculated on a weight-loss basis. The test exposures ranged from 2 to 9 days and up to 16 processing cycles. In an independent study of corrosion in simulated FBV processing conditions,[20] the higher corrosion rates in the fluidized bed were related to removal of the protective fluoride film by the action of the fluid-bed particles and also related to erosion effects, as outlined in Appendix A.

Type 304 and 347 stainless-steel coupons in the pyrohydrolysis reactor exhibited corrosion rates of less than 0.04 mil per day in the fluidized-bed region and above the fluidized bed. Inconel-600 exhibited only about 25% lower corrosion rates than the stainless steel in the pyrohydrolysis-reactor bed. Both Inconel and nickel sintered-metal filters were satisfactory for the pyrohydrolyzer off-gas. After a final cleaning with steam, the used filters exhibited pressure drops corresponding to those in new filters. Stainless-steel filters were not tested.

There was no evidence of gross dimensional changes in the reaction vessels other than slight distortion due to overheating and thermal cycling. Two diameter measurements on the stainless-steel pyrohydrolysis reactor were 6.077 and 6.026 in., which corresponded to 6.061- and 6.089-in. measurements as installed. Diametric distortions of up to 1/8 in. were measured for the 6-in.-diam nickel halogenation reactor. The distortion is apparently caused by local overheating in the regions near the tubular electrical heaters.

In isolated cases, specimens of nickel-200 and -201 exhibited a few areas in which apparent intergranular modifications have occurred ranging in depth from 1 to 2 mils. Data from the pilot-plant corrosion coupons and a discussion of the effects of corrosion on some of the equipment components are presented in Appendix B. The recommended materials of construction are summarized in Table IX.

TABLE IX. Recommended Materials of Construction for the FBV Processing of Uranium-Alloy Fuels

	Corrosive Environment	Recommended Material	Maximum Corrosion Rate (mil/day)
Halogenation Reactor and Packed-bed Filter	HCl, $ZrCl_4$, $AlCl_3$, H_2, HF, F_2, UF_6	Nickel-200 or -201	0.12
Pyrohydrolysis Reactor	HCl, $ZrCl_4$, $AlCl_3$, H_2, H_2O	Stainless steel or Inconel	0.04
Pyrohydrolyzer Filters	HCl, H_2O, H_2	Nickel or Inconel	-
Process Piping (A)	Dry HCl	Stainless steel	-
(B)	HF, F_2	Monel or nickel	-
(C)	HCl, $ZrCl_4$, $AlCl_3$, H_2, HF, F_2, UF_6	Nickel-200 or -201	0.09
(D)	Wet HCl above condensation point	Stainless steel or Inconel	0.04

VI. CONCLUSIONS

The operation of the pilot-plant facility with both the aluminum- and zirconium-based fuels has been satisfactory. High hydrochlorination rates and HCl-utilization efficiencies were achieved in the fluid-bed halogenation reactor by using 80 v/o HCl in nitrogen. The volatile metal chlorides were converted to solid oxide products, which appear suitable for waste disposal. The exothermic reaction of HCl with fuel elements was well-controlled by using a fluidized bed as a heat-transfer medium. The maximum fuel temperatures were 700°C for U-Zr fuels and 570°C for U-Al fuels, which are well below the melting points of the respective alloys. The packed-bed filter was effective for retaining uranium chlorides so that over 99% of the uranium was recovered in the fluorination of the halogenation-reactor and filter beds using the two-temperature fluorination procedures developed in the bench-scale work. Recoveries of over 99% of the input uranium as UF_6 on beds of NaF have been demonstrated.

Operation of the pilot plant has established certain design changes from the bench-scale recommendations for scale-up to full plant operation. Notable among these are the advisability of providing (1) a method for $FeCl_3$ or $AlCl_3$-$FeCl_3$ condensation upstream of the packed-bed filter during U-Al fuel processing, and (2) an efficient means of heat removal from the packed-bed filter during the fluorination step, i.e., fluidized fluorination of the bed particulate material. The success achieved in the pilot-plant and bench-scale[1,2] facilities has initiated a complementary study on irradiated fuels, which is now underway at ANL.[3]

The recommended operating conditions for high processing rates and high uranium recovery are as follows:

Bed Material:	High-fired alumina (fused or sintered) Halogenation-reactor fluid bed: Sufficient quantity of nominal -28, +100 mesh alumina to cover the fuel element (a multiplate assembly) Packed-bed filter: -14, +48 mesh alumina, >12 in. deep
Hydrochlorination:	Temperature of halogenation-reactor fluid bed: 350 to 450°C for U-Zr fuel, 300 to 350°C for U-Al fuel. Temperature of packed-bed filter: 330 to 350°C for U-Zr fuel and 180 to 200°C for U-Al fuel. Temperature of pyrohydrolysis reactor fluid bed: 350°C Gas velocity: 0.4 to 0.6 ft/sec in the fluid beds. Concentration of HCl in nitrogen: 80 v/o.

Fluorination:	Gradual increase in temperature of the halogenation-reactor fluid bed and packed-bed filter from 250 to 500°C while fluidizing with 1.0 to 5 v/o fluorine in nitrogen, then gradual increase in fluorine concentration to 60-80 v/o; the alumina particulate material may be maintained static during the later period. Total time: about 4 to 9.5 hr.

The FBV process offers the advantages of (1) simplified reprocessing of a variety of fuels, (2) high uranium recovery, (3) UF_6 product that can be isotopically enriched or converted directly back to fuel material, and (4) solid radioactive waste products.

APPENDIX A

Summary of Run Data

The pilot-plant run conditions and results are presented in the following three sections:

1. Run conditions and results (Tables X-XII)
2. Uranium balance (Table XIII)
3. Corrosion data.

1. Run Conditions and Results

TABLE X. Conditions and Results for Processing Zirconium-based Fuels

Run Number	Shakedown (Zr)			U-Zr Alloy Runs			
	1	2	6	7	13	14	15
Alloy Charge							
Fuel element (kg)	17.75	13.6	19.15	19.6 (14 plates)	12.72 (9 plates)	~21.0	20.380 (15 plates) 20.972 (16 plates) 15.038 (11 plates) 56.390
Uranium (g)	-	-	-	182.0 ± 4	117.0 ± 4	~160	546.0 ± 10
Hydrochlorination Data							
Average rate (kg/hr)	2.15	2.71	2.28	1.80	1.39	2.8	2.06
Maximum rate (kg/hr)	-	-	4.15	3.3	3.0	-	3.3
Reaction time (hr)	8.3	5.0	8.4	10.9	9.2	7.5	27.4 (9.1 per element)
Average HCl utilization (%)	40	43.0	36.2	24.4	22.1	-	33.5
Maximum HCl utilization (%)	-	-	66	46	53.0	-	59.0
Temperatures (°C)							
A. Hydrochlorination							
Reactor bed: Avg.	400	450	370	363	360	~395	372
Max.	450	545	405	380	388	408	403
Element channel: Avg.	-	490	374	390	370	~415	377
Max.	625	710	415	450	424	480	428
Halogenation-reactor wall	375	393	350	350	347	340	355
Packed-bed filter	380	390	388	360	346	360	365
Pyrohydrolysis-reactor bed	375	360	343	345	333	363	355
B. Hydrofluorination of 2 hr							
Halogenation-reactor bed	380	375	330	350	357	-	360
Filter bed	380	375	330	350	354	-	353
C. Fluorination							
Halogenation-reactor bed and filter							
(1) Reactor fluidized				250-500° (2.3 hr)	250-500° (6.2 hr)	250-500° (3.3 hr)	250-500° (2.5 hr)
(2) Reactor static				500° (1.5 hr)	500° (2.1 hr)	500° (3.8 hr)	500° (2.1 hr)
Reactant Concentrations (v/o)							
A. HCl in N_2	-	-	59	92	85	~80	79
B. HF in N_2				12	35	-	17.5
C. F_2 in N_2							
(1) Reactor fluidized				6.0	4.6	~5	4.6
(2) Reactor static				45.0	68	~70	68
Reactor Velocity (ft/sec)							
A. Hydrochlorination	0.6	0.72	0.59	0.53	0.44	~0.4	0.42
B. Hydrofluorination				0.5	0.38	-	0.49
C. Fluorination							
(1) Reactor fluidized				~0.6	0.40	~0.4	0.40
(2) Reactor static				~0.05	0.04	~0.04	0.04

TABLE XI. Conditions and Results for Processing Aluminum-based Fuels

Run Number	Shakedown (Al)			U-Al Alloy Runs							
	3	4	5	8	9	10	11	12	16	17	18
Alloy Charge											
Fuel element (kg)	13.65	12.1	12.3	6.060	6.195 6.150 6.166 18.511	6.030 6.080 5.971 18.081	5.880	5.962	6.025	6.127	5.965
Uranium (g)	-	-	-	273.6	841.3	828.7	280.4	280.5	273.6	289.0	280.0
Hydrochlorination Data											
Average rate (kg/hr)	1.17	1.64	1.92	1.09	1.48	1.26	0.86	0.96	0.88	0.90	0.94
Maximum rate (kg/hr)	1.9	2.6	3.24	1.6	3.0	1.6	1.3	2.8	1.4	1.4	1.5
Reaction time (hr)	11.6	7.4	6.4	5.6	12.5 (4.2 per element)	14.4 (4.8 per element)	6.8	6.5	6.9	6.8	6.3
Average HCl utilization (%)	54.6	50.4	41.4	40.0	48.3	52.6	37.2	37.4	43.2	45.5	45.4
Maximum HCl utilization (%)	90	80	90	60	90	65	56	65.0	66.6	72.0	69.1
Temperatures (°C)											
A. Hydrochlorination											
Reactor bed: Avg.	294	369	286	369	356	351	350	360	363	365	383
Max.	320	460	350	395	419	380	385	366	408	402	407
Element channel: Avg.	325	397	353	-	351	393	383	-	380	380	393
Max.	335	470	412	-	470	460	500	-	520	578	564
Halogenation-reactor wall	270	360	275	350	340	330	330	350	351	346	348
Packed-bed filter	297	336	287	296	183	190	190	197	335	255	250
Pyrohydrolysis-reactor bed	290	323	310	313	327	348	306	326	355	349	349
B. Hydrofluorination of 2 hr											
Halogenation-reactor bed	330	350	260	350	364	360	-	360	349	356	330
Filter bed	330	350	260	350	365	350	-	350	362	352	250
C. Fluorination											
Halogenation-reactor bed and filter											
(1) Reactor fluidized				250-500° (2.0 hr)	250-500° (2.8 hr)	250-500° (5.9 hr)	-	250-500° (7.5 hr)	250-500° (2.8 hr)	250-500° (2.2 hr)	250-500° (3.3 hr)
(2) Reactor static				500° (2.0 hr)	500° (2.1 hr)	500° (2.0 hr)	-	500° (2.0 hr)	500° (3.0 hr)	500° (4.1 hr)	500° (2.7 hr)
Reactant Concentrations (v/o)											
A. HCl in N_2	55	66	94	78	98	95	98	91	83.3	85.4	83.3
B. HF in N_2				8	26	27	-	21			
C. F_2 in N_2											
(1) Reactor fluidized				5.5	2.0	2.0	-	5	4.6	4.6	4.6
(2) Reactor static				40.0	40-60	30-50	-	68	68	68	68
Reactor Velocity (ft/sec)											
A. Hydrochlorination	0.54	0.50	0.56	0.54	0.48	0.40	0.39	0.39	0.40	0.38	0.36
B. Hydrofluorination				~0.5	~0.5	~0.5	-	0.41	0.5	0.5	0.5
C. Fluorination											
(1) Reactor fluidized				~0.6	~0.55	~0.50	-	0.39	0.40	0.40	0.40
(2) Reactor static				~0.05	~0.04	~0.04	-	0.04	0.04	0.04	0.04

TABLE XII. Pilot-plant Starting-bed Particulate Material

Run	Halogenation Reactor Bed				Packed-bed Filter				Pyrohydrolysis-reactor Bed			
	Wt. (kg)	Type[b]	Nominal Size (mesh)	Depth (in.)	Wt. (kg)	Type[b]	Nominal Size (mesh)	Depth (in.)[a]	Wt. (kg)	Type[b]	Nominal Size (mesh)	Starting Depth (in.)
1	40	RR alumina	60	51	-	38 alumina	20	-	20	Sand	25-60	26
2	40.6	RR alumina	60	52	9.0	38 alumina	20	4.5	20	Sand + ZrO_2 from run No. 1	-	-
3	38.0	T-61 alumina	28-100	49	9.0	T-61 alumina	14-28	4.5	16.5	T-61 alumina	28-100	28
4	40.0	T-61 alumina	28-100	51	9.0	T-61 alumina	14-28	6.5	21.5	Coarse from run No. 3	-	24
5	39.6	T-61 alumina	28-100	50	9.0	T-61 alumina	14-28	4.5	20.0	Bed from run No. 4	-	21.5
6	40.0	From run No. 5	28-100	51	9.0	T-61 alumina	14-28	5.5	19.2	New sand	25-60	~20
7	39.6	T-61 alumina	28-100	50	10.0	T-61 alumina	14-28	5.0	17.3	New sand	25-60	~18
8	40.0	T-61 alumina	28-100	51	15.5	T-61 alumina	14-28	6.5	15.9	38 alumina	60	~25
9	38.1	From run No. 8	28-100	49	15.2	T-61 alumina	14-48	12.0	20.2	T-61 alumina	48-100	~30
10	39.3	From run No. 9	28-100	50	15.6	T-61 alumina	14-48	12.0	4.9	Bed from run No. 9	-	-
11	40.0	T-61 alumina	28-100	51	14.0	T-61 alumina	14-48	11.0	10.0	T-61 alumina	28-48	~15
12	45.7	From run No. 10	28-100	58	13.1	T-61 alumina	14-48	10.0	10.0	Bed from run No. 10	-	~15
13	38.3	From run No. 7	28-100	49	16.0	T-61 alumina	14-48	11.5	10.0	T-61 alumina	28-48	~15
14	37.4	From run No. 13	28-100	48	15.0	T-61 alumina	14-48	11.5	10.0	T-61 alumina	28-48	~15
15	40.0	T-61 alumina	48-100	51	13.2	T-61 alumina	14-48	11.5	10.0	T-61 alumina	28-48	~15
16	43.3	From run No. 12	28-100	55	13.6	T-61 alumina	14-48	10.5	10.0	T-61 alumina	48-100	~15
17	42.2	From run No. 16	28-100	48	15.1	From run No. 16	14-48	11.0	10.0	T-61 alumina	48-100	~15
18	40.5	From run No. 17	28-100	52	15.4	T-61 alumina	14-48	11.5	10.0	T-61 alumina	48-100	~15

[a]Depth may vary because of amount of nickel balls in cone-shaped bottom.
[b]Type RR and 38 alumina were obtained from the Norton Co. Type T-61 was obtained from Alcoa.

2. Uranium Balance

TABLE XIII. Uranium Material Balance for Pilot-plant Runs

Run	7			13			14			15		
Fuel type	U-Zr			U-Zr			U-Zr			U-Zr		
Time @ 250-500°C	2.3			6.2			3.3			2.5		
(hr) @ 500°C	1.5			2.1			3.8			2.1		
HCl filter temperature, °C	360			346			360			365		
Filter depth (in.)	5.0			11.5			11.5			11.5		
No. of fuel elements	1			1			0.8			3		
	Wt. (g)	Total Wt. (g)	%	Wt. (g)	Total Wt. (g)	%	Wt. (g)	Total Wt. (g)	%	Wt. (g)	Total Wt. (g)	%
Charge		182 ± 4	100		117 ± 4	100		~160			546 ± 10	100
U Recoverable		179.7	98.7		108.9	93.0					582.5	106.7
NaF traps	176.4			106.6			-			579.7		
F_2 disposal	1.4			1.0			-			0.7		
Samples	1.9			1.3			-			2.1		
U Lost		7.1	3.9								11.6	2.1
Pyrohydrolysis reactor	4.7[d]		2.6[d]	0.3		0.2	0.25		0.2	4.4		0.8
Halogenation-reactor bed	1.4			5.7[r]		1.9	3.8[r]		0.8	4.3		0.8
Filter bed	0.9			1.5		1.3	1.6[r]		0.4	2.9		0.5
Scrubber	0.1			0.1		-	0.00		-	0.01		-
U Accounted for		186.8	102.6		116.7	99.7						

Run	8			9			10			9 and 10[f]			11		
Fuel type	U-Al			U-Al			U-Al			Filter beds			U-Al		
Time @ 250-500°C	2.0			2.8			5.9			2.0			*		
(hr) @ 500°C	2.0			2.1			2.0			2.0			*		
HCl filter temperature, °C	296			183			190			-			190		
Filter depth (in.)	6.5			12.0			12.0			-			11.0		
No. of fuel elements	1			3			3			0			1		
	Wt. (g)	Total Wt. (g)	%	Wt. (g)	Total Wt. (g)	%	Wt. (g)	Total Wt. (g)	%	Wt. (g)	Total Wt. (g)	%	Wt. (g)	Total Wt. (g)	%
Charge		273.6	100		841.7[r]	100		828.2[r]	100		5.86	100		280.4	100
U Recoverable		255.2	93.3		834.5[a]	99.1		744.8	89.9		3.75	64			
NaF traps	254.8			829.2			616.7						*		
F_2 disposal	0.32			2.2			126.6[i]						*		
Samples	0.1			3.1			1.5						*		
U Lost		15.0	5.5								2.1	36			
Pyrohydrolysis reactor	8.60[t,d]		3.1	3.17		0.38	4.45		0.54				1.9		<0.7
Halogenation-reactor bed	0.44		0.16	0.62[r]		0.056[b]	5.22[r]		0.27[b]				*		
Filter bed	5.9[c]		2.2	2.35[c]		0.28[c]	3.50[c]		0.42[c]	2.1		36	*		
Scrubber	0.003			0.02			0.05						0.00		
U Accounted for		270.2	98.8		840.7	99.9		758.0[i]	91.5						

TABLE XIII (Contd.)

Run	12			16			17			18		
Fuel type	U-Al			U-Al			U-Al			U-Al		
Time @ 250-500°C	7.5			2.8			2.2			3.3		
(hr) @ 500°C	2.0			3.0			4.1			2.7		
HCl filter temperature, °C	197			335			255			250		
Filter depth (in.)	10.0			10.5			11.0			11.5		
No. of fuel elements	1			1			1			1		
	Wt. (g)	Total Wt. (g)	%	Wt. (g)	Total Wt. (g)	%	Wt. (g)	Total Wt. (g)	%	Wt. (g)	Total Wt. (g)	%
Charge		285.7[r]	100		275.9[r]	100		292.3[r]	100		283.5[r]	100
U Recoverable		276.1	96.6		235	85.9		281.0	97.2		282.6	100.9
NaF traps	266.1			231.0			277.0			282.0		
F_2 disposal	49.7[i]			0.3			0.6			0.3		
Samples	0.3			3.7			3.4			0.3		
U Lost												
Pyrohydrolysis reactor	0.13		0.05	18.0[t]		6.6[t]	4.9[t]		1.7	4.2[t]		1.48
Halogenation-reactor bed	2.30[r]		0.099[b]	3.3[r]		0.13[b]	3.5[r]		0.08[b]	0.91[r]		0.03[b]
Filter bed	0.40[c]		0.14[c]	1.1		0.42	0.9[r]		0.16[b]	4.18[c]		1.48
Scrubber	0.01		-	0.008		0.00				0.00		-
U Accounted for		278.9[i]	97.6									

[d]Filter bed contained insufficient bed depth and too large particulate material.

[c]Caking occurred at the surface of the packed-bed filter.

[i]Inadvertent loss of UF_6 to the F_2 disposal system.

[r]Bed particulate material reused from the previous run; % is based on U charged in this run and in all prior runs.

*No fluorination step was performed.

[t]Filter-bed temperature too high: high U losses.

[b]Based on reuse of bed: total U charge from previous runs considered to get % loss.

[f]Refluorinated as fluidized beds reduced the loss in Runs 9 and 10.

[a]Does not include amount recoverable when filter bed was subsequently refluorinated.

3. Corrosion Data

a. Preparation and Analysis Procedures of Corrosion Coupons

The corrosion of the metals used in the pilot-plant construction and other metals that were considered as possible construction materials was investigated in the pilot-plant facility. Those investigated were nickel-200, nickel-201, Monel-400, Monel-K500, Inconel-600, Inconel-X750, and stainless steel Types 304 and 347.

The nickel, Monel, and Inconel corrosion coupons, cut from sheet material, were 0.025 in. thick; the nickel coupons used later in the program were 0.030 in. thick. Welded specimens were made by cutting a 1/2-in. piece from the end of a strip of 2.5-in. width, and welding the pieces together. Both welded and unwelded strips were cut into coupons of 1 x 2.5 in.

Nickel-200 and nickel-201 were welded with nickel-61 filler metal. Monel-400 used Monel-60 filler metal; Monel-K500 used Monel-64 filler metal. Inconel-600 was welded with Inconel-62 filler metal, and Inconel X-750 used Inconel-69 filler metal.

Stainless steel Type 304 was also studied. These coupons were made from sheet metal of 0.050-in. thickness; welded and unwelded coupons were made also of 1 x 2.5-in. size. The specimens of stainless steel Type 347 were 2-in. lengths of 3/8-in.-OD tubing.

After the coupons were cut to their appropriate size, holes were punched in them by which they could be suspended in the pilot-plant equipment. The coupons were then marked for identification by using a scribing tool. The edges were polished by means of a metallographic polishing wheel, first with 120 grit silicon carbide paper, and finally with 320 grit silicon carbide paper.

The specimens were then cleaned and degreased by using a Freon-acetone mixture and weighed by means of an analytical balance. The unwelded nickel and nickel-alloy coupons weighed approximately 9 g; the welded coupons weighed about 10 g. Both welded and unwelded coupons of stainless steel Type 304 weighed about 16 g; those of stainless steel Type 347 weighed 12 g.

These initial weights were recorded, and the coupons were then placed in the halogenation reactor, the packed-bed filter, and the pyrohydrolysis reactor in both the lower and upper portions of the units.

After being exposed in a number of runs, the coupons were removed and defilmed in a molten salt bath at 500°C for 30 min. The bath consisted of equimolar KNO_3-$NaNO_3$. The coupons were cooled immediately in water, and any smudge was removed with cleaning tissue. The coupons were weighed again on an analytical balance, and the corrosion rates were calculated. The corrosion rate for nickel was calculated as follows:

$$\text{mils/yr} = \frac{\text{g loss}}{\text{in}^2\ \text{hr}} \times \frac{\text{cm}^3}{8.91\ \text{g}} \times \frac{\text{in}^3}{(2.54\ \text{cm})^3} \times \frac{10^3\ \text{mils}}{\text{in.}} \times \frac{8760\ \text{hr}}{\text{yr}}.$$

b. Corrosion Results

After the corrosion rate was determined, the coupons were visually inspected and some specimens were selected for metallographic examination. The data are presented in Tables XIV-XX.

TABLE XIV. Corrosion-coupon Analyses

In the tables of corrosion data, the following abbreviations are used:

Abbreviation	Alloy Type	Weld Material
Ni-200	Nickel-200	Nickel-61 and nickel-200
Ni-201	Nickel-201	Nickel-61 and nickel-200
M-400	Monel-400	Monel-60
M-K500	Monel-K500	Monel-64
I-600	Inconel-600	Inconel-62
I-X750	Inconel-X750	Inconel-69
SS-304	304 stainless steel	304 stainless steel
SS-347	347 stainless steel	347 stainless steel

Chemical Composition of the Corrosion Coupon Alloys

	% Ni	% Cu	% Fe	% Cr	% Al	% Ti	% Mn	% C	% Si	% S	Nb + Ta	% Nb
Nickel-200	99.50	0.02	0.06	-	-	-	0.27	0.03	0.09	0.006	-	-
Nickel-201	99.60	0.02	0.07	-	-	-	-	0.02	0.02	0.005	-	-
Monel-400	64.49	33.38	0.84	-	-	-	0.95	0.12	0.19	0.007	-	-
Monel-K500	64.53	30.42	0.80	-	2.88	0.50	0.53	0.17	0.14	0.005	-	-
Inconel-600	75.84	0.12	7.50	15.95	-	-	0.22	0.04	0.30	0.007	-	-
Inconel-X750	73.74	0.06	6.46	14.92	0.75	2.35	0.54	0.03	0.24	0.007	0.88	-
Stainless-304	9.0	-	72.0	19.0	-	-	-	0.08	-	-	-	-
Stainless-347	10.0	-	71.0	18.0	-	-	-	0.1	-	-	-	0.8

The data obtained from coupons in the reaction system under actual processing conditions are given in Tables XV-XX.

TABLE XV. Data from Corrosion Coupons in Fluidized Section of Halogenation Reactor

	Process Cycles				Total Time (hr)	Corrosion Rate	
	Zr-based Fuels		Al-based Fuels				
	No.	hr	No.	hr		mil/yr	mil/day
Ni-200							
61	3	75.9			75.9	35.9[e]	0.098
62	3	75.9			75.9	37.8[e]	0.104
63	3	75.9			75.9	40.0[e]	0.110
64	3	75.9			75.9	42.0[e]	0.115
65	3	75.9			75.9	42.3[e]	0.116
66	3	75.9			75.9	40.8[e]	0.112
13W			4	83.6	98.2*	37.2[e]	0.102
23	4	95.6	6	118.8	229.0*	34.7[e]	0.095
Ni-201							
14			4	83.6	98.2*	30.1[e]	0.082
19	4	95.6	6	118.8	229.0*	30.8[e]	0.084
M-K500							
7			4	83.6	98.2*	38.3[e]	0.105

*Includes 14.6 hr of reagent only (no fuel element).

[e]Erosion effects as described in the text.

W indicates welded.

TABLE XVI. Data from Corrosion Coupons in Disengaging Section of Halogenation Reactor

	Process Cycles				Total Time (hr)	Corrosion Rate	
	Zr-based Fuels		Al-based Fuels				
	No.	hr	No.	hr		mil/yr	mil/day
Ni-200							
67	3	75.9			75.9	27.7	0.076
68	3	75.9			75.9	34.0	0.093
69	3	75.9			75.9	30.1	0.082
70	3	75.9			75.9	30.5	0.084
71	3	75.9			75.9	34.3	0.094
72	3	75.9			75.9	28.8	0.079
30	4	95.6	6	118.8	229.0*	17.4	0.048
1W	4	47.6	4	45.0	92.6	27.2	0.075
Ni-201							
9W			4	83.6	98.2*	10.0	0.027
13	4	95.6	6	118.8	229.0*	25.4	0.070
20	4	95.6	6	118.8	229.0*	20.2	0.055
M-400							
7W			4	83.6	98.2*	19.3	0.053
M-K500							
13			4	83.6	98.2*	14.7	0.040
11	4	95.6	6	118.8	229.0*	28.3	0.078

*Includes 14.6 hr of reagent only (no fuel element).
W indicates welded.

TABLE XVII. Data from Corrosion Coupons in Top Section of Packed-bed Filter

	Process Cycles				Total Time (hr)	Corrosion Rate	
	Zr-based Fuels		Al-based Fuels				
	No.	hr	No.	hr		mil/yr	mil/day
Ni-200							
52	3	75.9			75.9	34.9	0.096
53	3	75.9			75.9	35.1	0.096
54	3	75 9			75.9	39.4	0.108
51	3	75.9			75.9	38.1	0.104
33			4	83.6	98.2*	8.8	0.024
11W			4	83.6	98.2*	21.8	0.060
9W	3	75.9	5	103.2	193.7*	20.5	0.056
34	3	75.9	5	103.2	193.7*	19.4	0.053
6, 200W	3	75.9	5	103.2	193.7*	25.9	0.071
Ni-201							
21			4	83.6	98.2*	9.3	0.025
23			4	83.6	98.2*	10.5	0.029
22	3	75.9	5	103.2	193.7*	22.4	0.061
6W	3	75.9	5	103.2	193.7*	24.6	0.067

*Includes 14.6 hr of reagent only (no fuel element).
W indicates welded; 200W, welded with Ni-200.

TABLE XVIII. Data from Corrosion Coupons in Bottom Section of Packed-bed Filter

	Process Cycles				Total Time (hr)	Corrosion Rate	
	Zr-based Fuels		Al-based Fuels				
	No.	hr	No.	hr		mil/yr	mil/day
Ni-200							
47	3	75.9			75.9	31.6	0.087
48	3	75.9			75.9	30.2	0.083
49	3	75.9			75.9	32.6	0.089
50	3	75.9			75.9	32.7	0.090
35			4	83.6	98.2*	10.1	0.028
37			4	83.6	98.2*	6.1	0.017
36	3	75.9	5	103.2	193.7*	14.5	0.040
7, 200W	3	75.9	5	103.2	193.7*	42.0	0.115
5, 200W			4	83.6	98.2*	12.8	0.035
Ni-201							
24			4	83.6	98.2*	6.1	0.017
7W			4	83.6	98.2*	10.4	0.028
25	3	75.9	5	103.2	193.7*	19.7	0.054
26	3	75.9	5	103.2	193.7*	17.5	0.048

*Includes 14.6 hr of reagent only (no fuel element).
W indicates welded; 200W welded with Ni-200.

TABLE XIX. Data from Corrosion Coupons in Fluidized Section of Pyrohydrolysis Reactor

	Process Cycles				Total Time (hr)	Corrosion Rate	
	Zr-based Fuels		Al-based Fuels				
	No.	hr	No.	hr		mil/yr	mil/day
Ni-200							
56	3	44.1			44.1	13.3	0.036
57	3	44.1			44.1	15.1	0.041
20			4	58.0	64.3*	4.7	0.013
7W			4	58.0	64.3*	6.5	0.018
15	7	76.6	9	78.2	161.1*	11.1	0.030
M-400							
9W	3	44.1			44.1	18.3	0.050
I-600							
8W	3	44.1			44.1	8.0	0.022
7			4	58.0	64.3*	4.5	0.012
16	7	76.6	9	78.2	161.1*	4.0	0.011
17	7	76.6	9	78.2	161.1*	5.7	0.016
I-X750							
11			4	58.0	64.3*	1.9	0.005
10	7	76.6	9	78.2	161.1*	2.3	0.006
SS-304							
6	3	44.1			44.1	10.9	0.030
8	3	44.1			44.1	14.4	0.039
1W			4	58.0	64.3*	6.0	0.016
4			4	58.0	64.3*	5.8	0.016
SS-347							
12	3	44.1			44.1	11.8	0.032
3			4	58.0	64.3*	3.7	0 010
2	7	76.6		78.2	161.1*	5.3	0.015
4	7	76.6		78.2	161.1*	4.5	0.012
6	7	76.6		78.2	161.1*	2.8	0.008

*Includes 6.3 hr of reagent only (no fuel element).
W indicates welded.

TABLE XX. Data from Corrosion Coupons in Top Section of Pyrohydrolysis Reactor

	Process Cycles				Total Time (hr)	Corrosion Rate	
	Zr-based Fuels		Al-based Fuels				
	No.	hr	No.	hr		mil/yr	mil/day
Ni-200							
55	3	44.1			44.1	5.2	0.014
19			4	58.0	64.3*	1.3	0.004
6	7	76.6	9	78.2	161.1*	32.0	0.088
6W	7	76.6	9	78.2	161.1*	2.8	0.008
M-400							
8W	3	44.1			44.1	3.3	0.009
10			4	58.0	64.3*	2.2	0.006
14	7	76.6	9	78.2	161.1*	3.6	0.010
4W	7	76.6	9	78.2	161.1*	4.3	0.012
I-600							
6W	3	44.1			44.1	0.6	0.002
10			4	58.0	64.3*	0.6	0.002
3W			4	58.0	64.3*	0.9	0.002
15	7	76.6	9	78.2	161.1*	2.9	0.008
18	7	76.6	9	78.2	161.1*	1.6	0.004
I-X750							
19	3	44.1			44.1	0.5	0.001
13			4	58.0	64.3*	0.6	0.002
7	7	76.6	9	78.2	161.1*	1.3	0.004
9	7	76.6	9	78.2	161.1*	1.2	0.003
4W	7	76.6	9	78.2	161.1*	1.4	0.004
SS-304							
5	3	44.1			44.1	8.3	0.023
1			4	58.0	64.3*	1.9	0.005
2	7	76.6	9	78.2	161.1*	14.1	0.039
7	7	76.6	9	78.2	161.1*	6.4	0.018
2W	7	76.6	9	78.2	161.1*	5.3	0.015
SS-347							
9	3	44.1			44.1	6.3	0.017
8			4	58.0	64.3*	2.2	0.006
1	7	76.6	9	78.2	161.1*	6.0	0.016
11	7	76.6	9	78.2	161.1*	6.8	0.019

*Includes 6.3 hr of reagent only (no fuel element).
W indicates welded.

The corrosion rates reported for the fluid-bed region are higher than the rates obtained for coupons that were above the fluid bed. In these tests, the higher rates were due to two causes: (1) the scrubbing action of the fluid bed partially removes the protective nickel fluoride film, and (2) corrosion proceeds at a faster rate. Figure 12 illustrates how the reactor basket is scrubbed "clean" in the fluid-bed region (bottom) and how the region above the fluid bed (top) has an adhering fluoride film. Part of the higher rates are also due to erosion effects, as illustrated in Fig. 13. The erosion was caused by the swinging of the coupon on its support due to the turbulent nature of the fluid bed. Stationary parts of the system, such as thermocouple wells, did not exhibit similar gross erosion effects; therefore erosion is not expected to be a problem for a normally operating system.

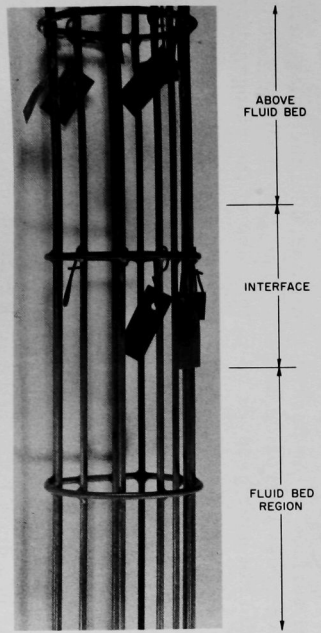

108-7743A

Fig. 12. Halogenation-reactor Basket and Corrosion Coupons

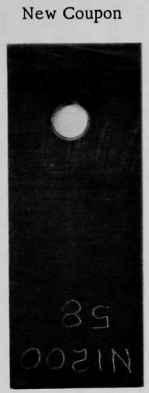

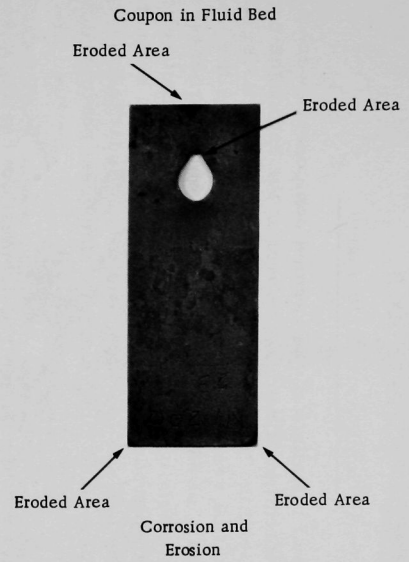

108-8383T

Fig. 13. Pilot-plant Corrosion Coupons

APPENDIX B

Component Performance

At the time of installation, the various components were accurately measured with the intention of remeasurement at the end of the experimental runs in order to determine the amount of gross corrosion taking place on the walls of the reaction vessels. An attempt to remeasure the inside diameters of the reactors showed that the heating and cooling processes had caused the vessels to be slightly distorted in diameter so that reliable corrosion measurements could not be obtained. Corrosion evaluation of the inside of the reactors was therefore limited to visual inspection of these surfaces, which is described along with the component performance in the following discussion.

The preheater met the design requirements of heating gaseous HCl, HF, and F_2 from ambient temperature to 350°C for HCl and HF, and up to 500°C for fluorine. No preheating failures occurred during any of the 18 runs made with the equipment.

The halogenation reactor had no interior areas that indicated gross corrosion after the 18 runs. This vessel had a nickel fluoride film of up to 1/32-in. thickness, which was acting as a protective film. The walls adjacent to the fluidized bed had significantly thinner protective films. The bubble-cap gas distributor was covered by a film of nickel fluoride and alumina fines (see Fig. 14). The four gas-outlet holes in each bubble cap were still circular in shape, with no signs of gross erosion or corrosion. Some soft lumps of alumina fines were lodged between the bubble caps (see Fig. 15). The plug valve in the solids exit pipe under the reactor did not show signs of metal galling, even though the Teflon liner had metal and alumina particles embedded in its surface (see Fig. 16). No leakage was experienced with this valve. The gasket surface on the top charge port of the reactor was slightly grooved (see Fig. 17). Even with the grooves present, the port was sealed without leakage of process gases.

The internal surface of the packed-bed filter, like the halogenation reactor, did not have gross corrosion damage. The gasket surface on the filter charge port did not have grooves as in the case of the halogenation reactor.

The interior of the pyrohydrolysis reactor did not show visual signs of corrosion as a result of exposure to gaseous HCl, H_2, steam, $ZrCl_4$, and $AlCl_3$ at 350°C. The 60° cone-shaped gas distributor at the bottom of the reactor had some discolored areas (see Fig. 18), but no gross corrosion or pitting was evident. The seat at the bottom of the cone (Fig. 19) had some eroded areas. When the $1\frac{1}{4}$-in.-diam stainless-steel ball rested against the seat, the gas distributor had a leak rate of approximately 1.0 cfm at 10 psig pressure, which is considered satisfactory. At the end

108-8218A

Fig. 14. Bubble-cap Gas Distributor for Halogenation Reactor

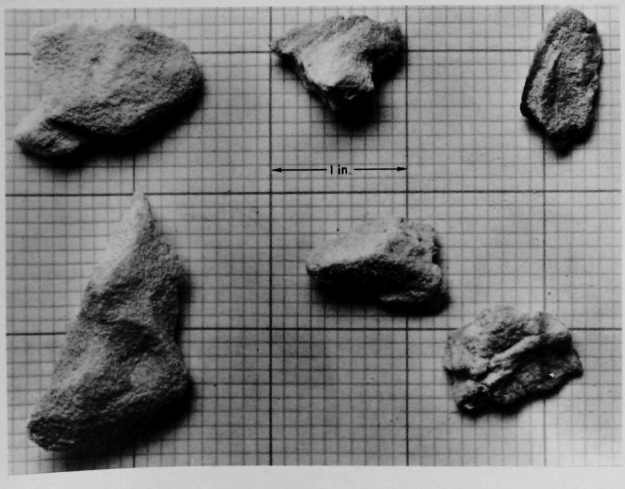

Fig. 15

Lumps of Alumina Found between Bubble Caps

108-8185A

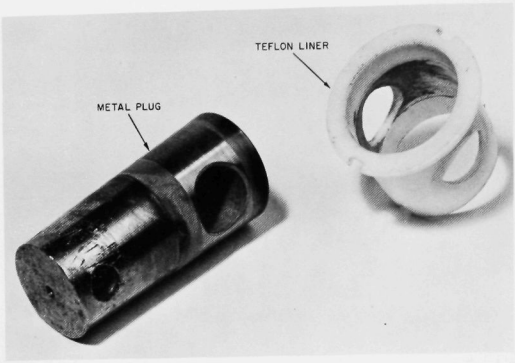

Fig. 16

Teflon-lined Plug Valve

108-8181A

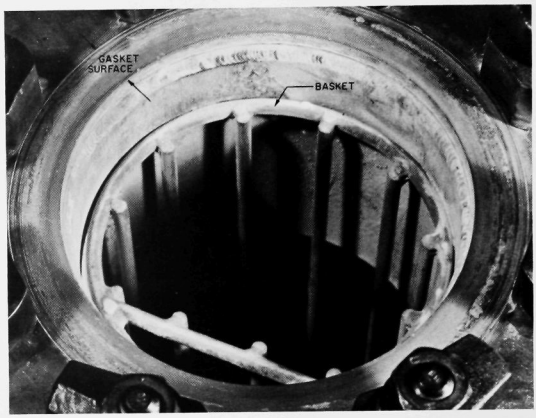

Fig. 17

Halogenation-reactor Charge Port and Top of Basket

108-8314A

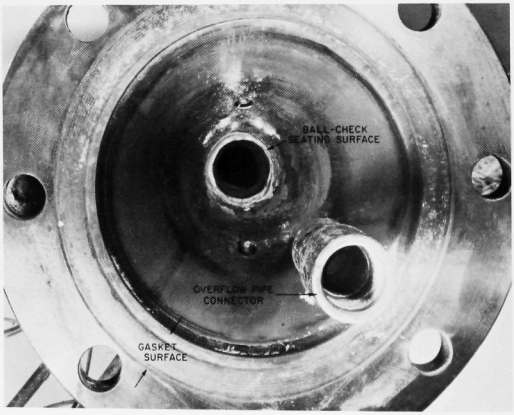

Fig. 18

Pyrohydrolysis-reactor Cone-shaped Gas Distributor

108-8188A

108-8186A

Fig. 19. Pyrohydrolysis-reactor Cone-shaped Gas Distributor, Showing Detail of Seating Area for $1\frac{1}{4}$-in.-diam Ball Check

of the last run, the ball was still of a spherical shape, within 0.0005 in., at a final diameter of 1.155 in. compared to a starting diameter of 1.250 in. (see Fig. 20). Erosion, rather than corrosion, probably caused the size reduction. This effect indicates that the ball would require regular replacement. The erosion or corrosion of the steam nozzle is illustrated in Fig. 21 by comparing the shape of the hole in the used steam nozzle with the hole in an unused nozzle. The used nozzle (on the right) was considered to be performing in a satisfactory manner throughout the 18 runs. The sintered-metal filters as shown in Fig. 22 indicate the amount of zirconium or aluminum oxide which collected during the course of one run--about 1/16 in. in thickness. This film

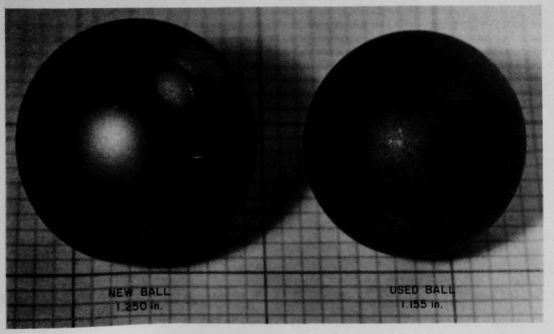

108-8183A

Fig. 20. Stainless-steel Balls Used in Pyrohydrolysis-reactor Cone-shaped Gas Distributor

adhered firmly enough to the metal filter so the nitrogen blow-back did not completely remove it. The four filters (two nickel and two Inconel) were removed from the cover plate, brushed, and tested for pressure drop. The Inconel filters had higher pressure drops than similar new filters; however, all four of the used filters were considered satisfactory. Each filter was cleaned for an hour by using a reverse flow of steam from the inside to the outside of the filter. The pressure drops of the four filters were then checked against a similar new filter. Pressure drops across both nickel and Inconel filters were found to be essentially equal to those of new filters. Metallographic examination showed no gross changes between the new and used filters. Sintered stainless-steel filters may also be applicable but were not tested in this study.

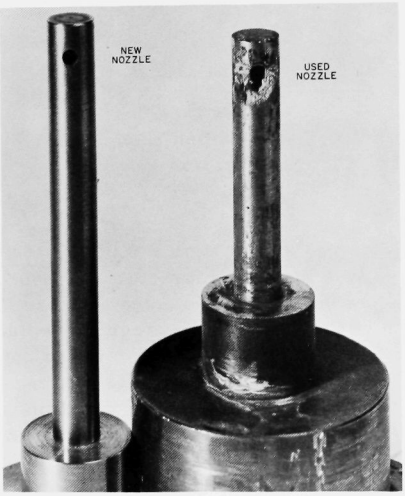

108-8190A

Fig. 21. Pyrohydrolysis-reactor Steam Nozzles

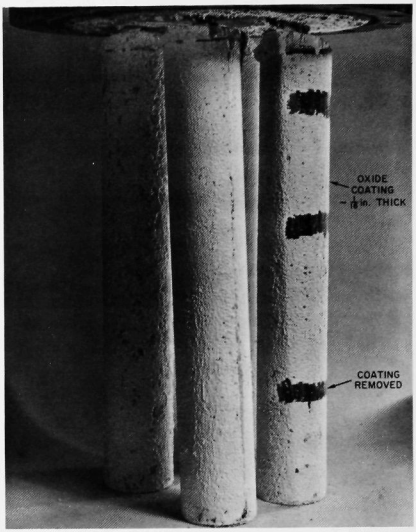

108-8216A

Fig. 22. Pyrohydrolysis-reactor Sintered-metal Filters

The two fluorine-disposal columns, of Monel, which were operated with a maximum wall temperature of 250°C, did not show any serious effects of corrosion. A tightly-adhering fluoride scale, observed on the inside surface, probably acted as a protective coating.

During the series of 18 runs, the air-operated valves used to direct and control the process flow rates occasionally developed in-line leaks, which resulted from an accumulation of fine powder (ZrO_2 or Al_2O_3) on the valve seats. Figure 23 shows the accumulation of fines on a Teflon seat,

which did not cause significant in-line leakage; yet the high-temperature valve plug shown in Fig. 24 did have an excessive in-line leak rate due to a build-up of fines. A 1/32-in.-thick deposit on the sides of the metal plug in the high-temperature valve caused binding with the close-fitting valve body. No trouble was experienced with binding of the valve in Fig. 23 because of greater clearances and the use of a pilot guide for the seating surfaces. The slight groove on the metal valve plug shown in Fig. 25 did not cause the valve to leak significantly. The valve seat in Fig. 26 has a new Teflon seat. The broken Teflon seat at the side became brittle and translucent after 24 hr of intermittent exposure to hydrogen fluoride at approximately 150°C.

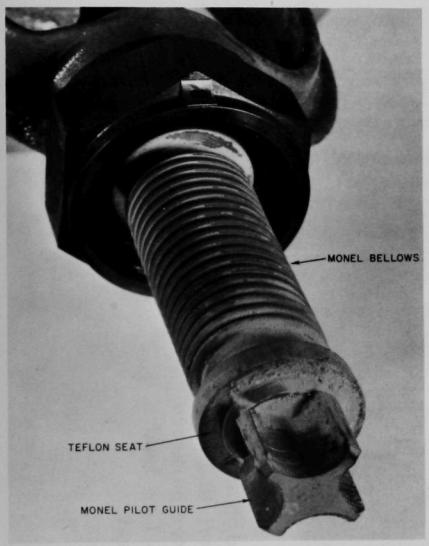

108-8210A

Fig. 23

Large, Bellows-sealed, Monel Valve with Teflon Seat

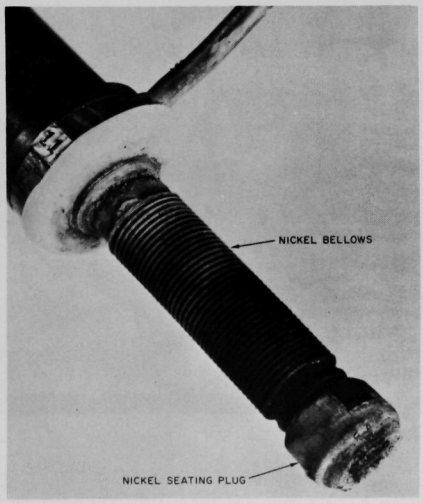

108-8213A

Fig. 24

Bellows-sealed, Nickel Valve with Metal-to-Metal Seat for High-temperature Operation with High Leak Rate across Seat

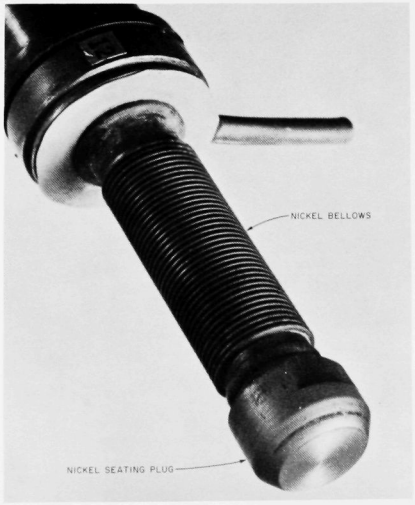

108-8212A

Fig. 25. Bellows-sealed, Nickel Valve with Metal-to-Metal Seat for High-temperature Operation with Low Leak Rate across Seat

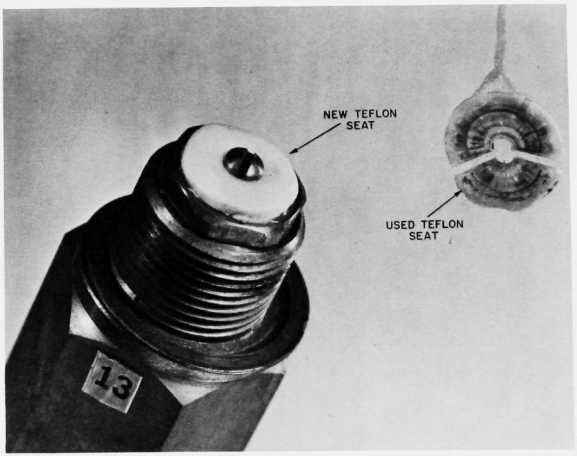

108-8211A

Fig. 26. Small, Bellows-sealed, Monel Valve with Teflon Seat Exposed to HF at 150°C

Certain improvements became obvious when routine maintenance operations were performed on the equipment while the pilot plant was being operated during 18 experimental runs. The most important of these improvements are:

1. The piping between the halogenation reactor and the packed-bed filter should slope down toward reactor to prevent hold-up of particulate solids.

2. All piping connections should be made with flanges, rather than pipe unions, as were used in a number of spots in the pilot plant.

3. Valves should be designed with clearance between valve-seat pilot guide and pilot hole sufficient to minimize binding effects from fine powders. Additional effort should be made to keep fine powders out of lines containing valves.

4. Steam cleaning of the sintered-metal filters should be performed periodically. This may be accomplished routinely by using steam as the blow-back gas.

5. The packed-bed filter should be sized to accommodate a bed depth of over 12 in.

6. The packed-bed filter should be designed so that the bed material can be fluidized during the fluorination step if necessary.

APPENDIX C

Continuous Off-gas Analysis

The hydrochlorination reaction was continuously monitored with a thermal-conductivity cell by measuring the concentration of hydrogen in the off-gas. The system is similar to the one described by Ramaswami[1] and is shown schematically in Fig. 27.

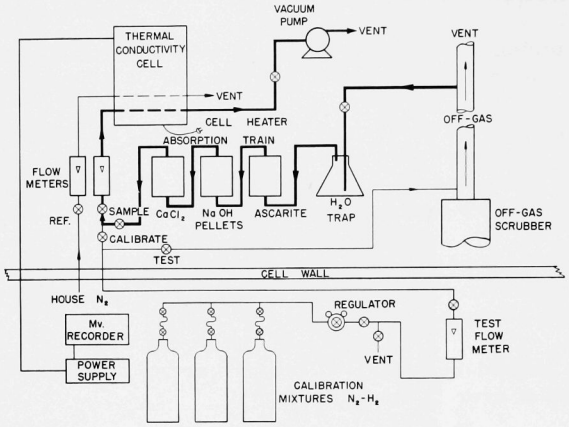

108-8269

Fig. 27. Thermal-conductivity Apparatus Used for Nitrogen-Hydrogen in FBV Pilot Plant

The calibration and operation of the thermal-conductivity apparatus consisted of four major parts: (1) The absorption train was renewed and leak-tested before establishing the initial base-line reading (nitrogen sample vs nitrogen reference). (2) Calibration was then performed by using known concentrations of nitrogen and hydrogen as the sample gas. (3) The system was then tested by introducing a quantity of hydrogen to a nitrogen stream, which actually flowed through the pilot-plant equipment. (4) The actual run data were then accumulated when the hydrochlorination reaction was initiated. This procedure produced a consistently accurate monitor of the HCl reaction rate, utilization efficiency, and pyrohydrolysis reaction rate.

The fluorination reaction was followed qualitatively by means of a thermal-conductivity system like the one described by Ramaswami,[1] except that a reference gas of pure nitrogen was compared to the mixture of F_2, N_2, and UF_6 at a location preceding the sodium fluoride traps.

ACKNOWLEDGMENTS

The authors wish to thank R. C. Vogel, M. Levenson, A. A. Jonke, N. M. Levitz, D. Ramaswami, A. A. Chilenskas, and K. S. Turner for their cooperation and interest in the project. Thanks are also due to C. B. Schoffstoll and W. A. Kremsner, who shared the major operating responsibility, and to R. P. Larsen, L. E. Ross, and their associates, who performed the analytical support work.

REFERENCES

1. D. Ramaswami, N. M. Levitz, J. T. Holmes, and A. A. Jonke, Engineering Development of Fluid-bed Fluoride Volatility Processes, Part 1. Bench-scale Investigation of a Process for Zirconium-Uranium Alloy Fuel, ANL-6829 (Dec 1964).

2. D. Ramaswami, N. M. Levitz, and A. A. Jonke, Engineering Development of a Fluid-bed Fluoride Volatility Process for High Enriched Uranium Alloy Fuels, Part 2. Bench-scale Investigation of a Process for Aluminum-Uranium Alloy and Stainless Steel Cermet Fuel, ANL-6830, to be published (1965).

3. A. A. Chilenskas and K. S. Turner, Engineering Development of Fluid-bed Fluoride Volatility Processes, Part 10. Bench-scale Studies on Irradiated Highly-enriched Uranium Alloy Fuels, ANL-6994, to be published.

4. F. Patton, J. Googin, and W. Griffith, Enriched Uranium Processing, p. 9, Pergamon Press, New York (1963).

5. The Shippingport Pressurized Water Reactor, Addison-Wesley Publishing Company, Inc., Reading, Massachusetts (1958).

6. A. A. Jonke, V. H. Munnecke, R. C. Vogel, and S. Vogler, Process for Recovering Uranium from Zirconium-Uranium Fuel, TID-10089 (Feb. 24, 1954) pp. 7-12.

7. G. Cathers, R. Jolley, and E. Moncrief, Laboratory-Scale Demonstration of the Fused Salt Volatility Process, Nucl. Sci. Eng. (13): 391-397 (1962).

8. W. Mecham, R. Liimatainen, R. Kessie, and W. Seefeldt, Decontamination of Irradiated Uranium by a Fluoride Volatility Process, Chem. Eng. Prog. (53): 72F-77F (1957).

9. P. Faugeras, Treatment of Irradiated Fuel by Volatilization of Fluorides, Symposium on Aqueous Reprocessing Chemistry for Irradiated Fuel, Brussels, AEC-tr-5811 (April 23-26, 1963).

10. C. Johnson, J. Stockbar, and W. Gunther, Chemical Engineering Division Summary Report for April, May, June 1961, ANL-6379 (1961), pp. 146-157.

11. J. Rielly, W. Regan, E. Wirsing, and L. Hatch, Uranium Recovery from Unirradiated Reactor Fuel Elements. Volatile Separation in Inert Fluidized Beds, Ind. Eng. Chem., Process Design Develop. 2(2): 127-133 (April 1963).

12. C. Williams and F. T. Miles, Progress Report, Nuclear Engineering Department, May to August 1960, BNL-646 (S-56), p. 18.

13. M. Bourgeois and P. Nollet, Study of the Chemical Treatment of Uranium-Zirconium Fuels by Volatility, French Report, CEA-R-2508 (1964).

14. M. Bourgeois and P. Faugeras, The Processing of Irradiated Fuels by the Halogens and Their Compounds, presented at the Third United Nations Conference on the Peaceful Uses of Atomic Energy, Geneva, 1964, Paper A/Conf. 28/P/66.

15. M. Bourgeois, Treatment of Irradiated Fuels by Non-aqueous Methods, Bull. Inform. Sci. Tech. (Paris). No. 66: 65-72 (Nov 1962).

16. K. S. Sutherland and D. J. Raue, Chemical Engineering Division Summary Report for April, May, and June 1963, ANL-6725 (1963) pp. 183-184.

17. J. T. Holmes and D. Ramaswami, Engineering Development of Fluid-bed Fluoride Volatility Processes, Part 9. Computer Programs for Alloy Fuel Process Calculations, ANL-6992, to be published.

18. N. Levitz, J. Barghusen, and J. Holmes, Chemical Engineering Division Summary Report for January, February, and March 1963, ANL-6687 (1963), pp. 147-149.

19. K. N. Semenenlso, T. N. Naumova, L. N. Gorokhov, G. A. Semenova, and A. V. Novoselova, Interactions of the Chlorides of Al and Fe, Proc. Acad. Sci. USSR, Chem. Sect. 154 (1-6): 42-43 (Jan-Feb 1964).

20. A. A. Chilenskas and G. E. Gunderson, Engineering Development of Fluid-bed Fluoride Volatility Processes, Part 7. The Corrosion of Nickel in Process Environments, ANL-6979, Argonne National Laboratory (March 1965).